The Abdus Salam International Centre for Theoretical Physics

United Nations Educational, Scientific and Cultural Organization

IAEA International Atomic Energy Agency

2066-3

Workshop and Conference on Biogeochemical Impacts of Climate and Land-Use Changes on Marine Ecosystems

2 - 10 November 2009

Introduction to ocean color remote sensing (theory and data sources)

A. Subramaniam

LDEO
Columbia University
U.S.A

Strada Costiera 11, 34151 Trieste, Italy - Tel.+39 040 2240 111; Fax +39 040 224 163 - sci_info@ictp.it

Introduction to ocean color remote sensing
Part 1 - theory and data sources

Ajit Subramaniam
ajit@ldeo.columbia.edu
Lamont Doherty Earth Observatory
Columbia University

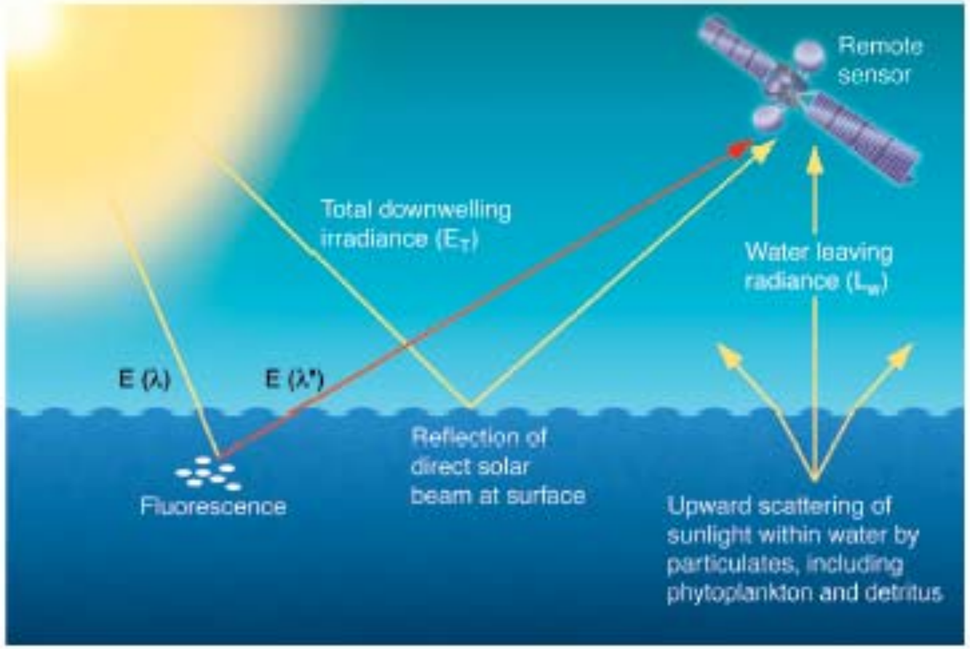

The color of the ocean is recorded by a satellite sensor by measuring the "remote sensing reflectance (R_{rs})" at specific wavelengths. R_{rs} is the ratio of light leaving the water (L_w) to the light incident on it (E_T) and is determined by the absorption (a) and backscattering (b_b) of light in the water column ($R_{rs} = L_w/E_T \propto b_b/(a + b_b)$).

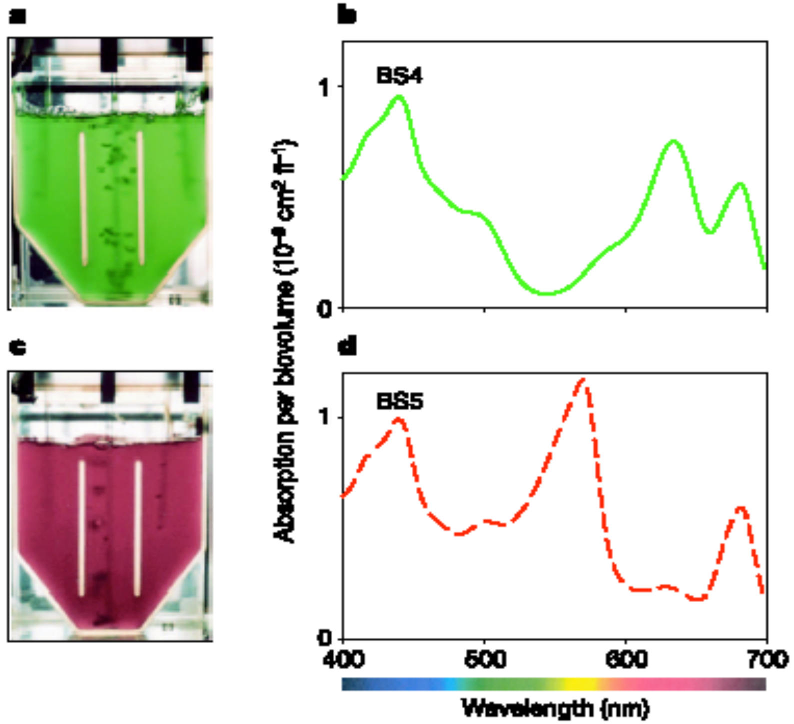

Figure 1 Optical characteristics of the picocyanobacteria BS4 and BS5. Monocultures of BS4 (**a**) and BS5 (**c**) grown in chemostats, and the light absorption spectra of BS4 (**b**) and BS5 (**d**).

Reflectance model for Chl=10 mg/m^3

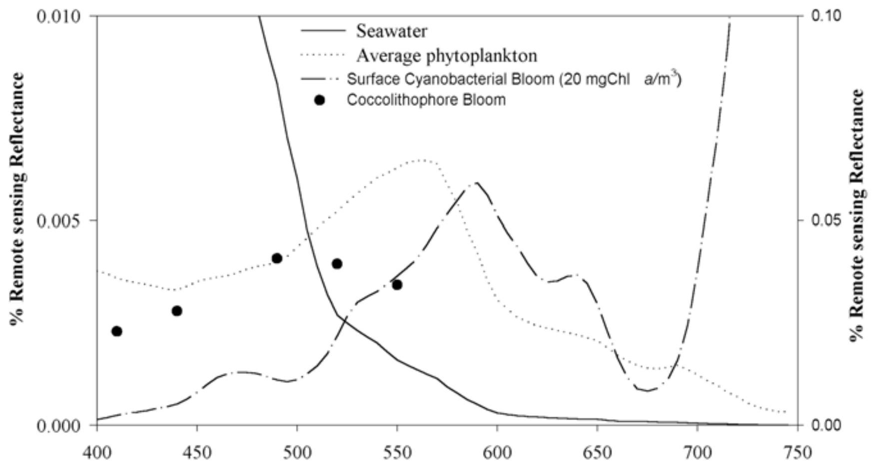

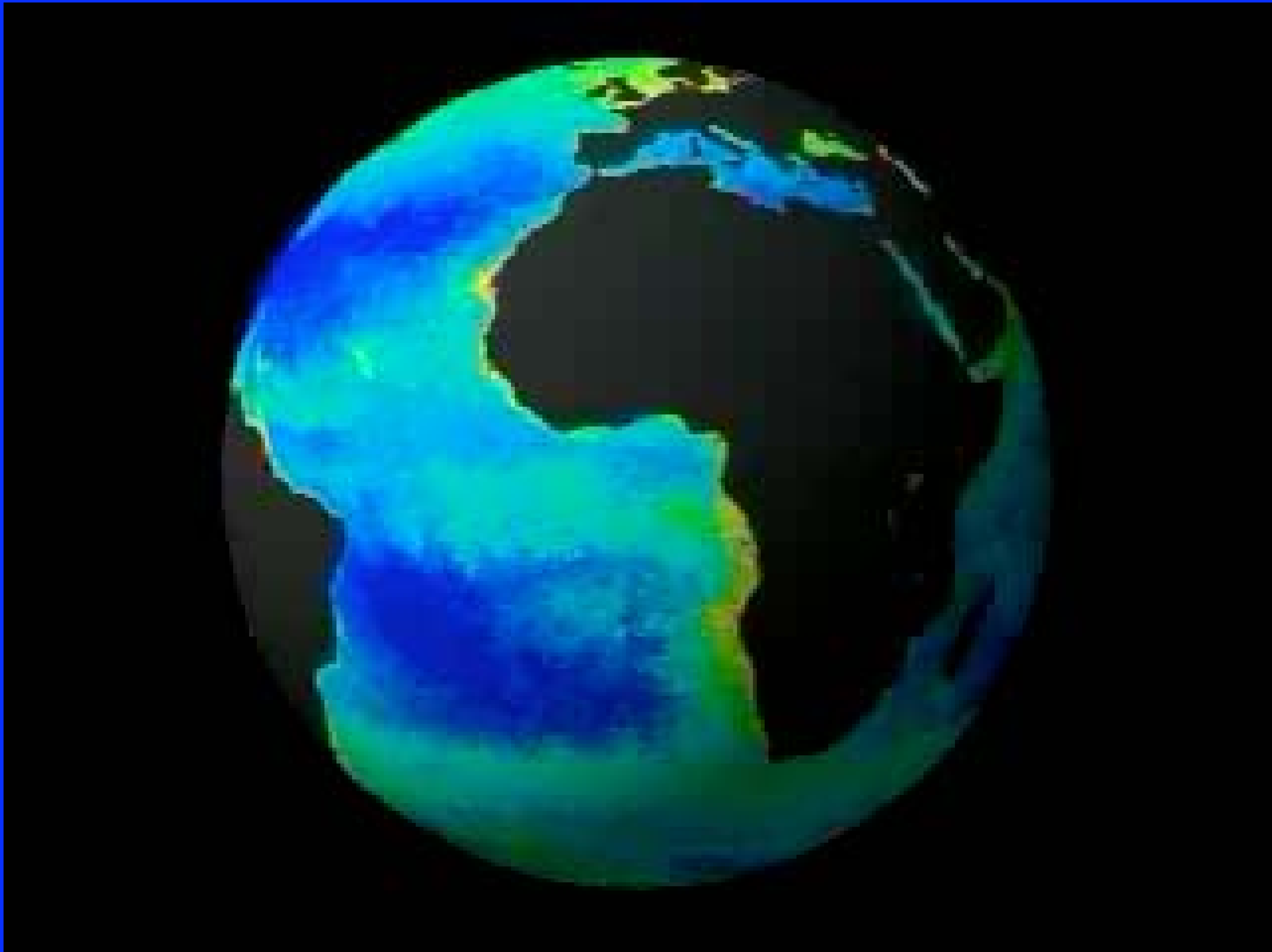

- The use of remote sensing, ocean optics, knowledge of phytoplankton physiology, biological and physical oceanography and geographical information systems to better understand and manage the coastal marine ecosystem

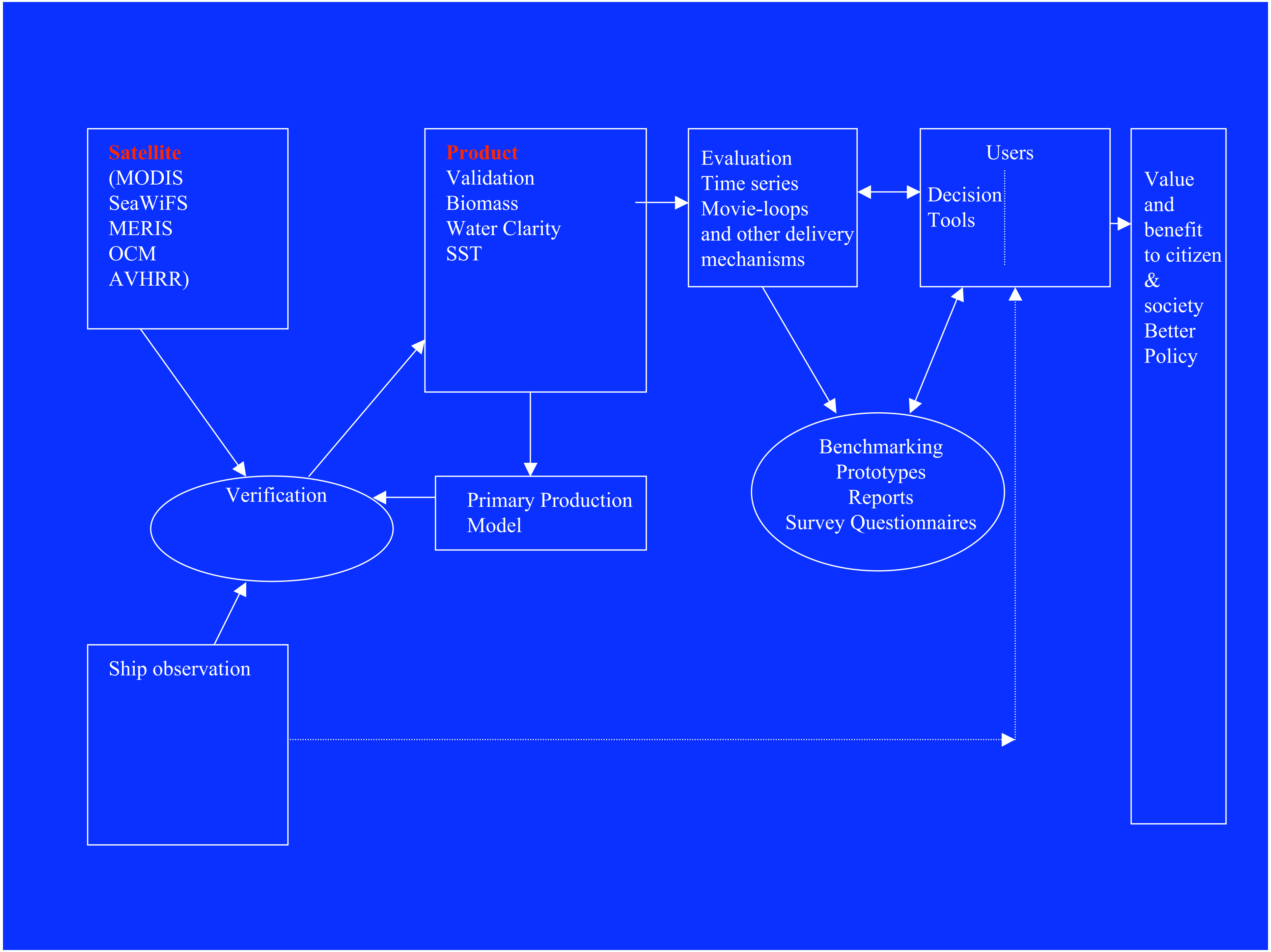
Satellite
(MODIS
SeaWiFS
MERIS
OCM
AVHRR)
Product
Validation
Biomass
Water Clarity
SST
Evaluation
Time series
Movie-loops
and other delivery
mechanisms
Users
Decision
Tools
Value
and
benefit
to citizen
&
society
Better
Policy
Verification
Primary Production
Model
Benchmarking
Prototypes
Reports
Survey Questionnaires
Ship observation

- Once placed in service, satellites provide regular, regionally synoptic data that can complement conventional shipboard surveys by filling the gaps between surveys.

- Satellite based sensors can be a very cost effect method for collecting environmental data.

- Remote sensing techniques can be used to monitor coastal water quality

•Regional synoptic data can help distinguish between nearfield and farfield effects and separate local production from that advected into the region.

•Satellite sensors can also be a continuous source of information for decadal scale monitoring of the dynamics of natural and anthropogenic changes in the ecosystem, often providing baseline data for "before" and "after" conditions.

•We will go over the basic principles of bio-optics to understand and interpret satellite data and how to validate it with field data

A term project for the final class grade that would require the processing, analysis, display, and interpretation of ocean color data.

The students will form two person teams for a total of six projects

Come up with ideas for projects that have a clear application and validation datasets needed for it.

AVHRR 1986 and 1999, Averages

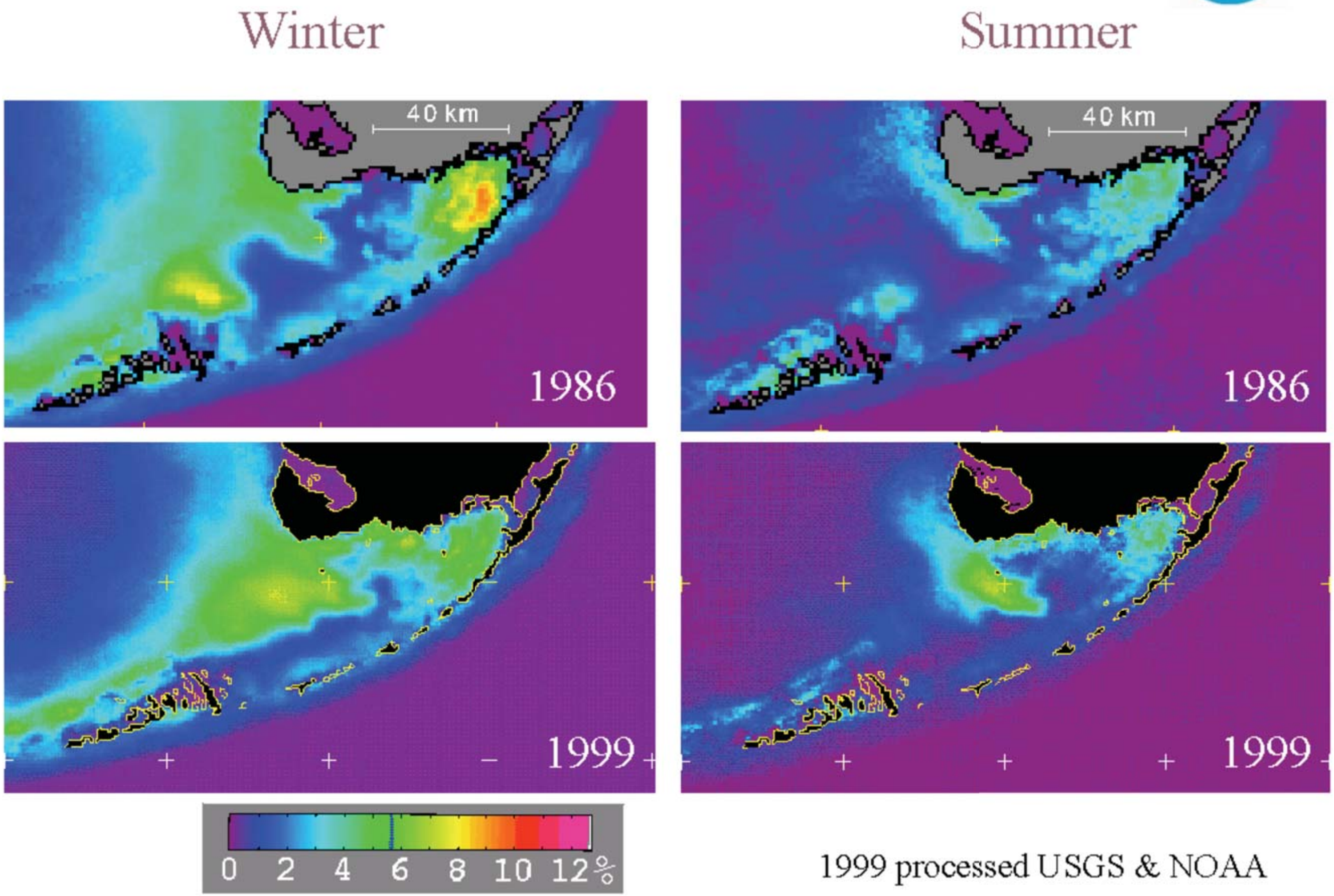

1999 processed USGS & NOAA

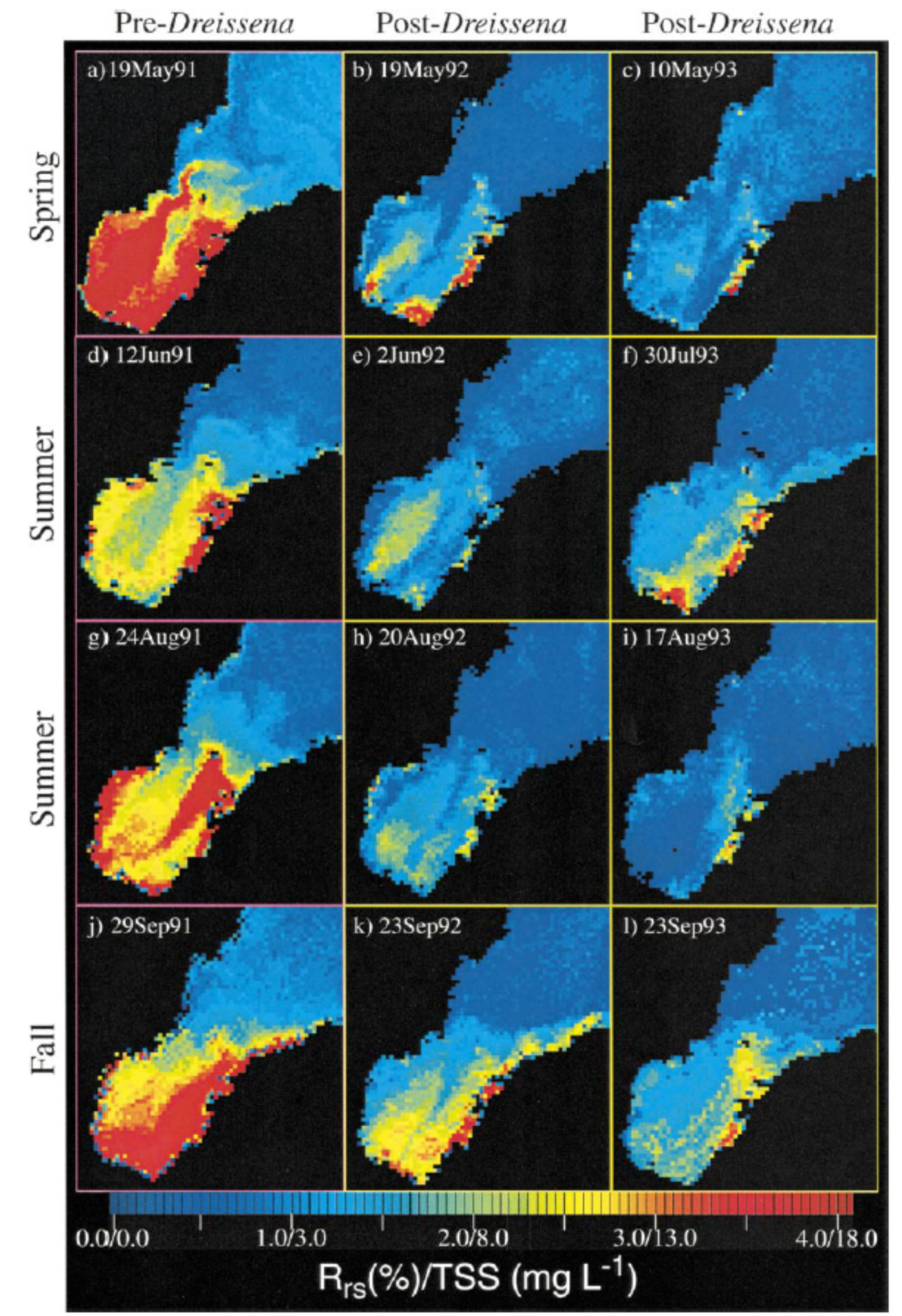

Spatial and temporal trends in the data indicate distinct and persistent increases in water clarity in the inner bay after the first large recruitment of zebra mussels in the fall of 1991. The pre-*Dreissena* imagery show that turbidity in the inner bay was influenced by the Saginaw River discharge in spring, phytoplankton in summer, and wind-driven resuspension in fall. Spatial patterns in the post-*Dreissena* images were more similar regardless of season, with low reflectances in the shallow regions of the inner bay where zebra mussel densities were highest.
Budd et al. 2001 Limnol. Oceanogr., 46(2), 213–223.

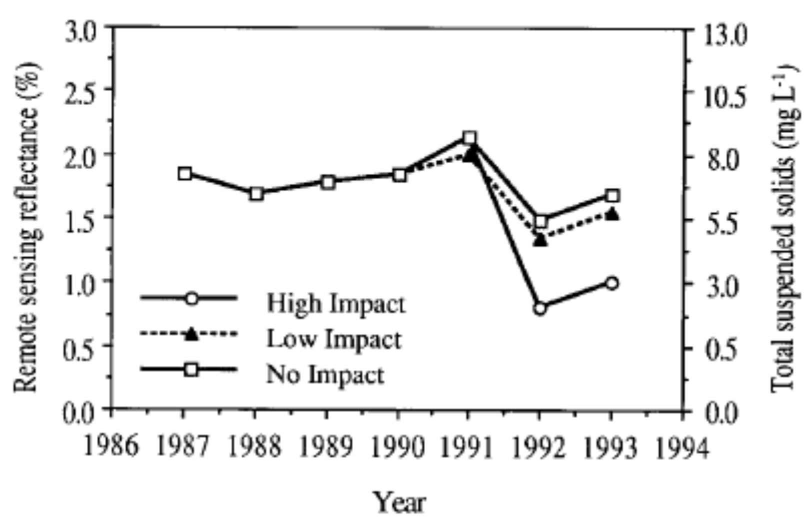

Fig. 5. Model-based changes in reflectance for average high-, low-, and no-density stations by year during midsummer (day of year = 200 or July 19).

Hot Button Issues in Coastal Zone

- **Water quality/ human health**
- **Hypoxia**
- **HABs**
- **Invasive species**
- **Fish farms**
- **Dredging**
- **Climate change/ Greenhouse gases**

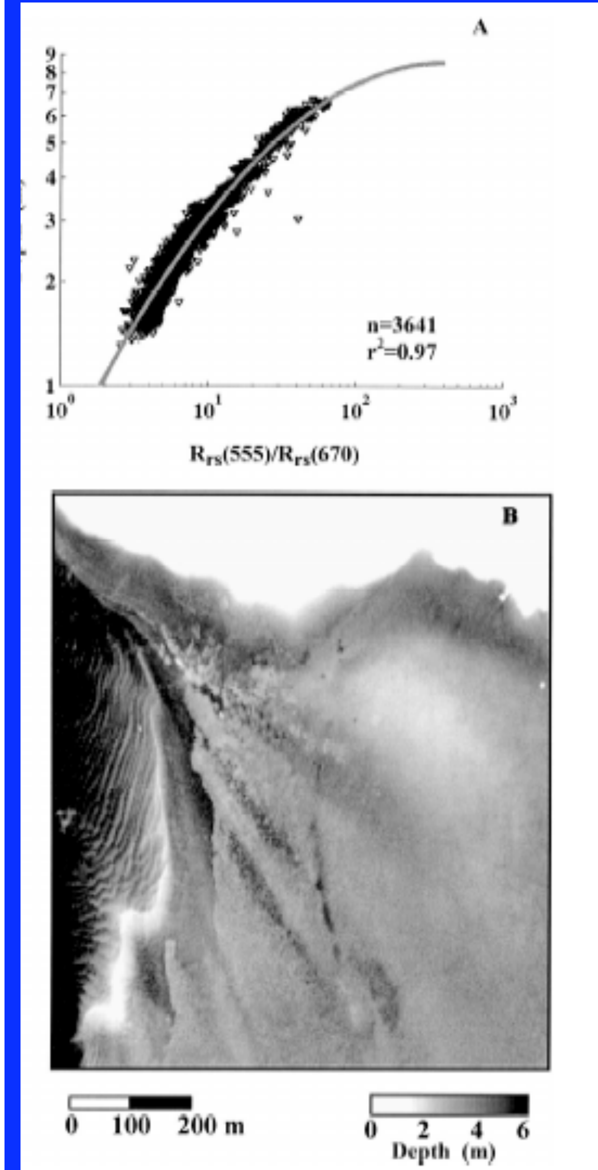

(A) Relationship between bottom depth and ratio of Rrs(555)/ Rrs(670). (B) Remotely sensed bathymetry estimated using the PHILLS 99 data.

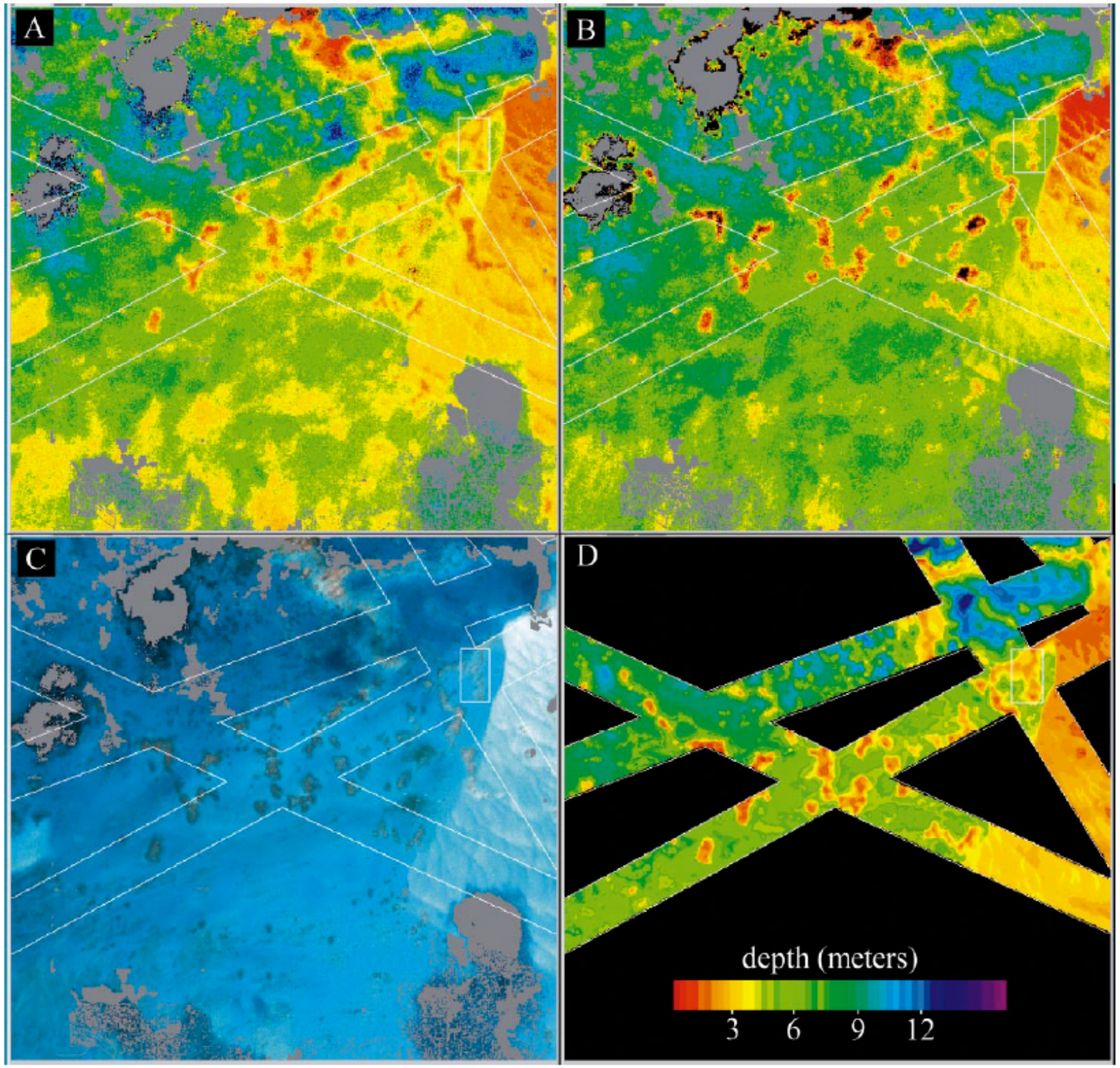

Fig. 7. Depths from the three methods and "true-color" water reflectance for central Kure: (A) ratio, (B) linear, (C) true-color, and (D) lidar. The lidar swaths are 200 m wide and marked on each image. Depths are shown in meters with scale bar at lower right. The box (at upper right in each image) marks a patch reef of low reflectance. IKONOS imagery courtesy of Space Imaging.

Deer Island #29,627 May 26, 2000

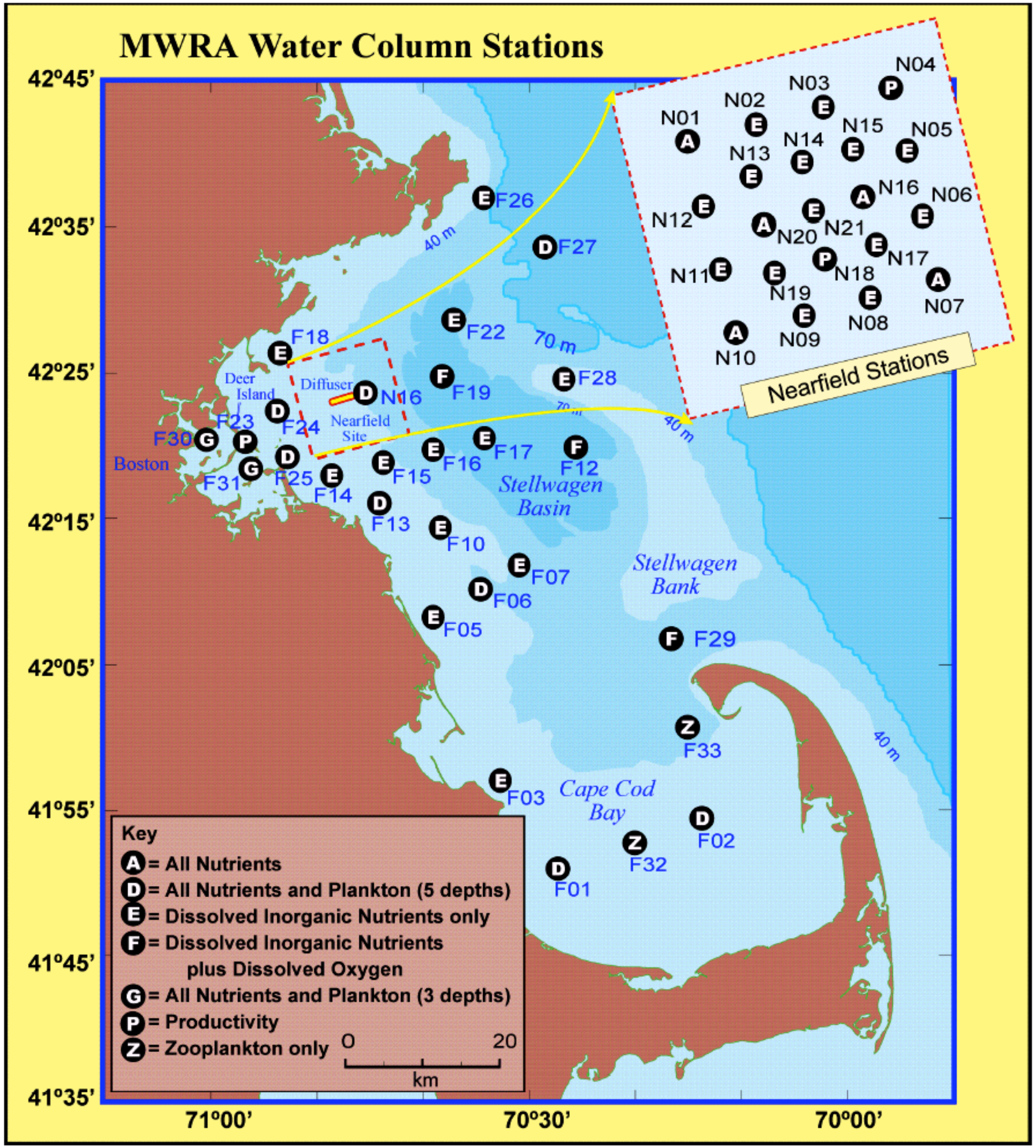
MWRA Water Column Stations
42°45'
42°35'
42°25'
42°15'
42°05'
41°55'
41°45'
41°35'
71°00'
70°30'
70°00'
Nearfield Stations
N01 N02 N03 N04 N05 N06 N07 N08 N09 N10 N11 N12 N13 N14 N15 N16 N17 N18 N19 N20 N21
F01 F02 F03 F05 F06 F07 F10 F12 F13 F14 F15 F16 F17 F18 F19 F22 F23 F24 F25 F26 F27 F28 F29 F30 F31 F32 F33
Deer Island
Diffuser
Nearfield Site
Boston
Stellwagen Basin
Stellwagen Bank
Cape Cod Bay
40 m
70 m
Key
A = All Nutrients
D = All Nutrients and Plankton (5 depths)
E = Dissolved Inorganic Nutrients only
F = Dissolved Inorganic Nutrients plus Dissolved Oxygen
G = All Nutrients and Plankton (3 depths)
P = Productivity
Z = Zooplankton only
0 20
km

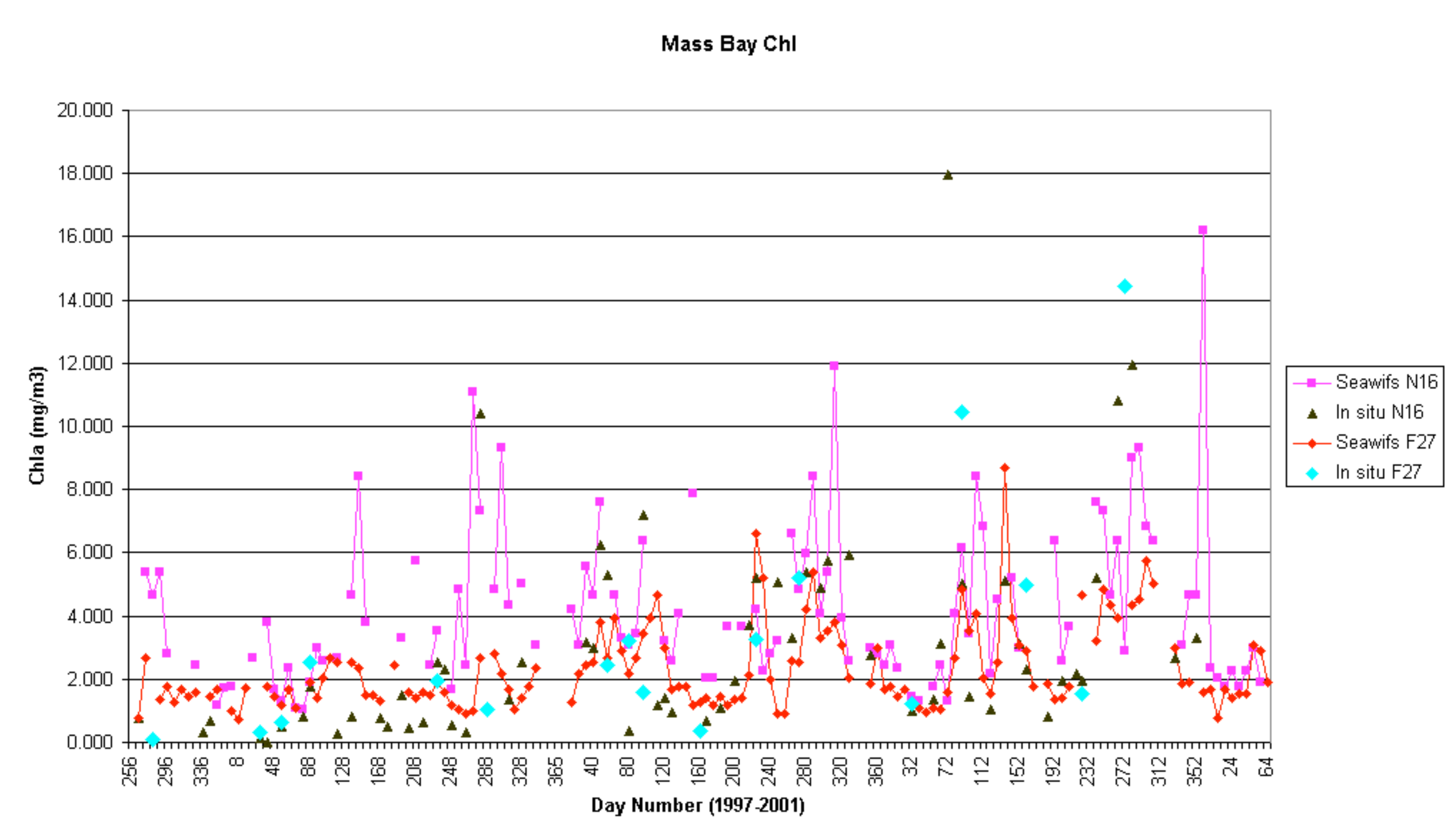

Mass Bay Chl
Chla (mg/m3)
20.000
18.000
16.000
14.000
12.000
10.000
8.000
6.000
4.000
2.000
0.000
256
296
336
8
48
88
128
168
208
248
288
328
365
40
80
120
160
200
240
280
320
360
32
72
112
152
192
232
272
312
352
24
64
Day Number (1997-2001)
Seawifs N16
In situ N16
Seawifs F27
In situ F27

0 Days	F02	N16	F26	GoMOOS
F02	1	**0.20**	**0.20**	**0.14**
N16		1	**0.55**	**0.41**
F26			**1**	**0.52**
GoMOOS				**1**

-8 Days	F02	N16	F26	GoMOOS
F02	**0.43**	**0.18**	**0.12**	**0.16**
N16	**0.07**	**0.30**	**0.31**	**0.43**
F26	**0.17**	**0.43**	**0.46**	**0.37**
GoMOOS	**0.16**	**0.30**	**0.42**	**0.46**

-16 Days	**F02**	N16	F26	GoMOOS
F02	**0.25**	0.06	0.04	0.22
N16	0.09	**0.24**	.018	0.15
F26	**0.15**	**0.28**	**0.24**	**0.21**
GoMOOS	**0.14**	**0.22**	**0.22**	**0.25**

Values in bold are 95% significant

The GoMOOS B Buoy site is significantly correlated 8 days ahead of N16.

1998-1999

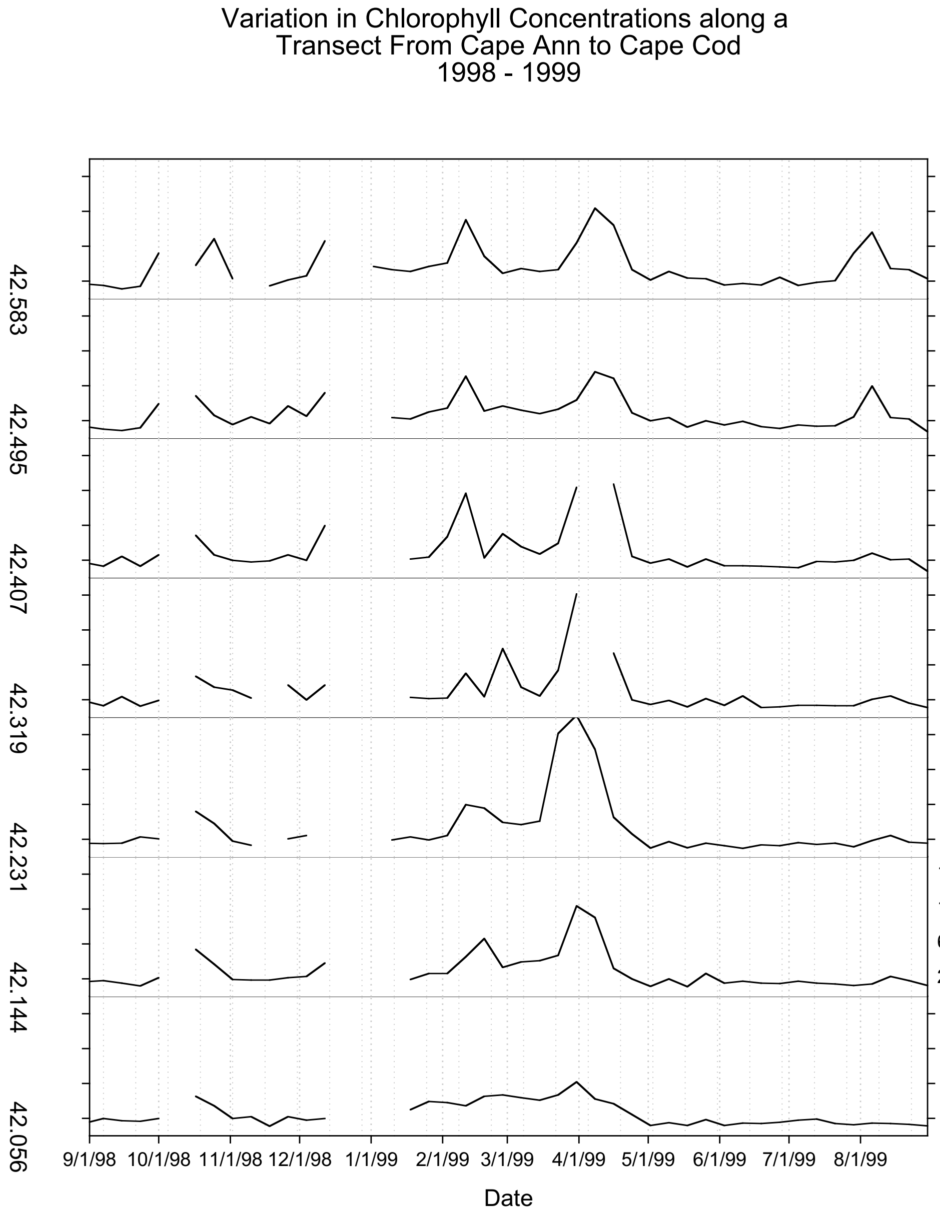
Variation in Chlorophyll Concentrations along a
Transect From Cape Ann to Cape Cod
1998 - 1999
42.583
42.495
42.407
42.319
42.231
42.144
42.056
14
10
6
2
9/1/98 10/1/98 11/1/98 12/1/98 1/1/99 2/1/99 3/1/99 4/1/99 5/1/99 6/1/99 7/1/99 8/1/99
Date

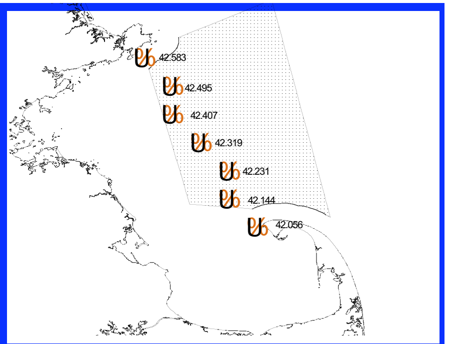
42.583
42.495
42.407
42.319
42.231
42.144
42.056

What is ocean color?

Remote sensing of the visible part of the electromagnetic spectrum

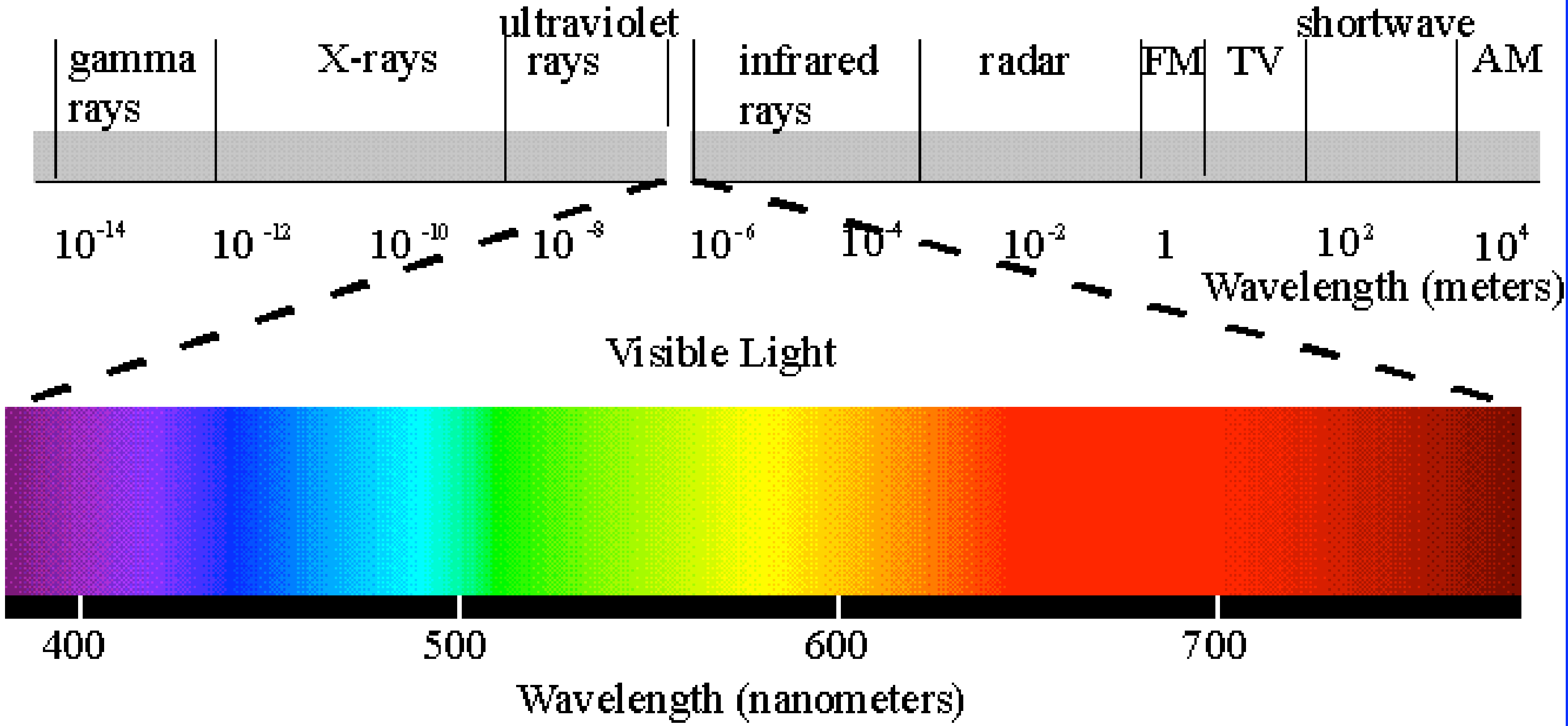

Table of Contents

Visual Stimulus

What is ocean color?

Remote sensing of the visible part of the electromagnetic spectrum

- AVHRR 1979 – present (~ 1km,
- SPOT 1986 – present (20m, 500-590, 610-680)
- Landsat
  - MSS 1972-1983 (30m, 500-600, 600-700)
  - TM 1982-present (30m, 450-520, 520-600, 630-690)
- GOES 1975 – present (~1 km, 550-750)
- Meteosat 1977 – present (2.4 km, 400-1100, 570-710)

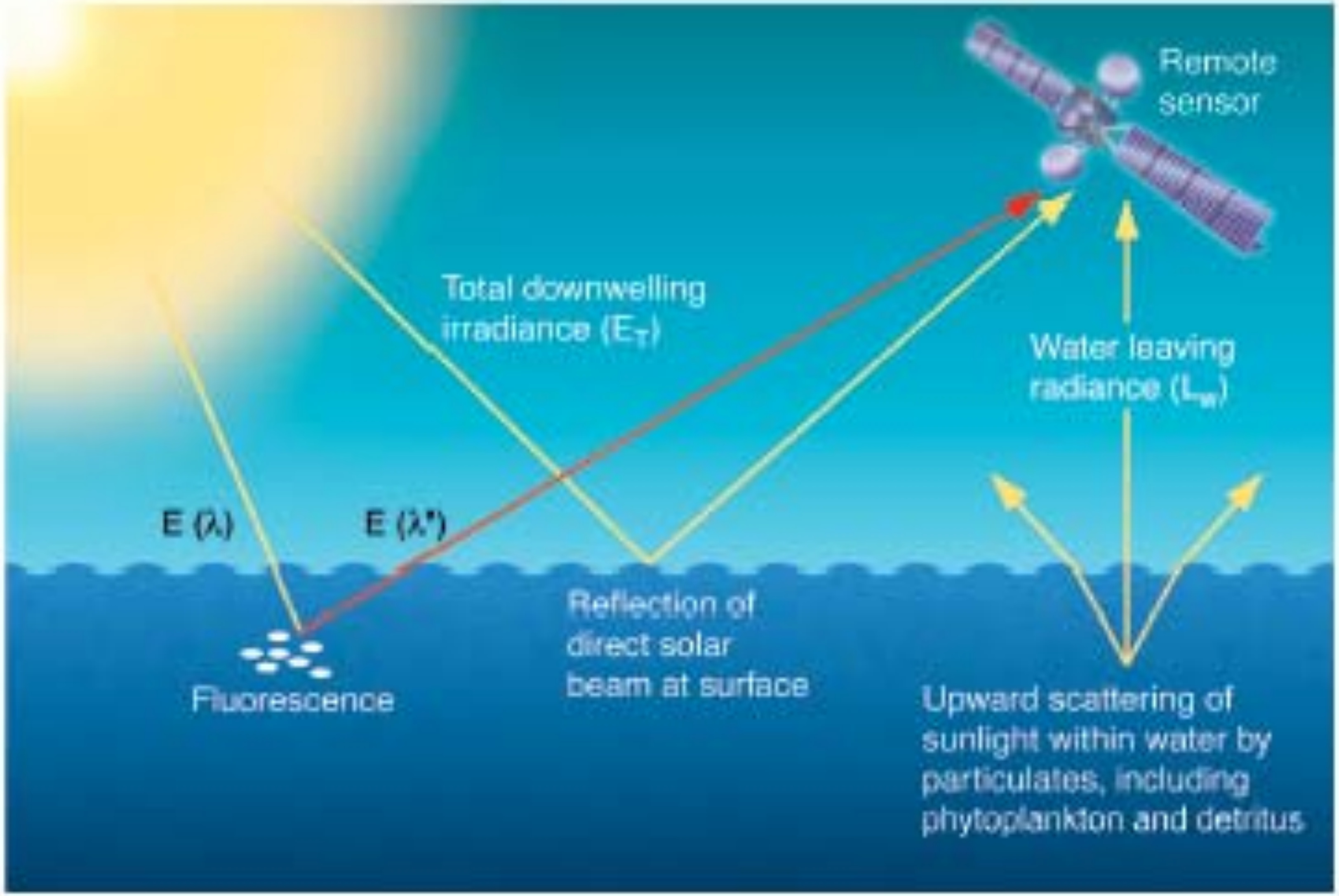

The color of the ocean is recorded by a satellite sensor by measuring the "remote sensing reflectance (R_{rs})" at specific wavelengths. R_{rs} is the ratio of light leaving the water (L_w) to the light incident on it (E_T) and is determined by the absorption (a) and backscattering (b_b) of light in the water column ($R_{rs} = L_w/E_T \propto b_b/(a + b_b)$).

Historical Ocean-Color Sensors

Sensor	Agency	Satellite	Operating Dates	Swath (km)	Resolution (m)	# of Bands	Spectral Coverage (nm)
CZCS	NASA (USA)	Nimbus-7 (USA)	10/24/78-06/22/86	1556	825	6	433-12500
MOS	DLR (Germany)	IRS P3 (India)	03/21/96-05/31/04	200	500	18	408-1600
OCTS	NASDA (Japan)	ADEOS (Japan)	08/17/96-07/01/97	1400	700	12	402-12500
Polder	CNES (France)	ADEOS (Japan)	08/17/96-07/01/97	2400	6000	9	443-910
CMODIS	CNSA (China)	Shen Zhou-3	03/25/02-09/15/02	-	400	34	403-12500
CZI	CNSA (China)	Hai Yang-1	05/15/02-12/01/03	500	250	4	420-890
GLI	NASDA (Japan)	ADEOS II (Japan)	12/14/02-10/25/03	1600	250/1000	36	375-12500
Polder II	NASDA (Japan)	ADEOS II (Japan)	12/14/02-10/25/03	2400	6000	9	443-910

Current and Future Ocean-Color Sensors

Sensor	Agency	Satellite	Operating Dates	Swath (km)	Resolution (m)	# of Bands	Spectral Coverage (nm)
SeaWiFS	NASA (USA)	OrbView-2 (USA)	08/1997	2806	1100	8	402-885
OCI	NSPO (Taiwan)	ROCSAT-1 (Taiwan)	01/1999	690	825	6	433-12500
OCM	ISRO (India)	IRS-P4 (India)	05/1999	1420	350	8	402-885
OSMI	KARI (Korea)	KOMPSAT (Korea)	12/1999	800	850	6	400-900
Terra	NASA (USA)	MODIS	12/1999	2330	1000	36	405-14385
MERIS	ESA (Europe)	Envisat –1 (Europe)	03/2002	1150	300/1200	15	412-1050
Aqua	NASA (USA)	MODIS	05/2002	2330	1000	36	405-14385
COCTS	CNSA (China)	HaiYang-1 (China)	05/2002	1400	1100	10	402-12500

Trichodesmium colonies

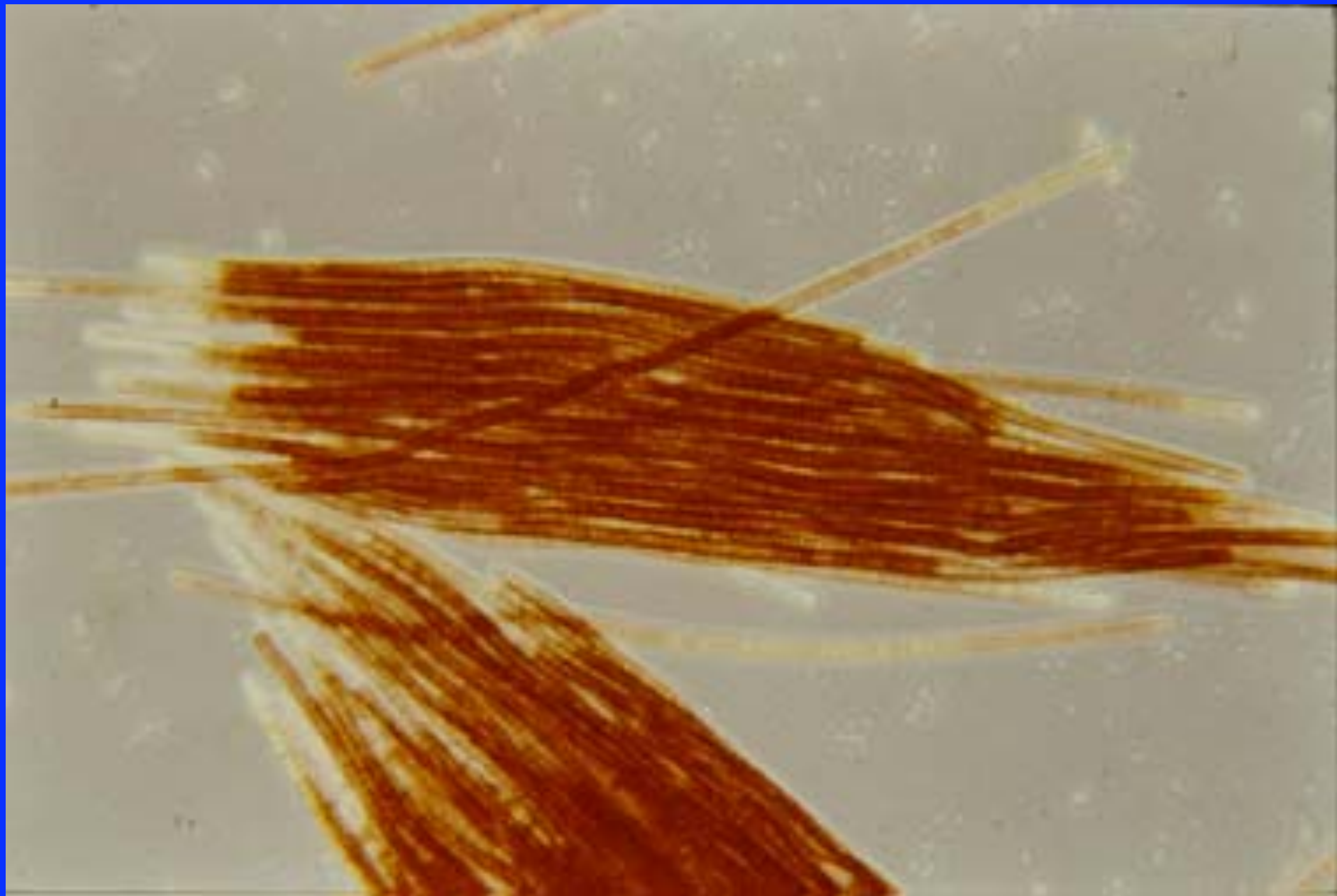

Tricho slick

Space shuttle photo

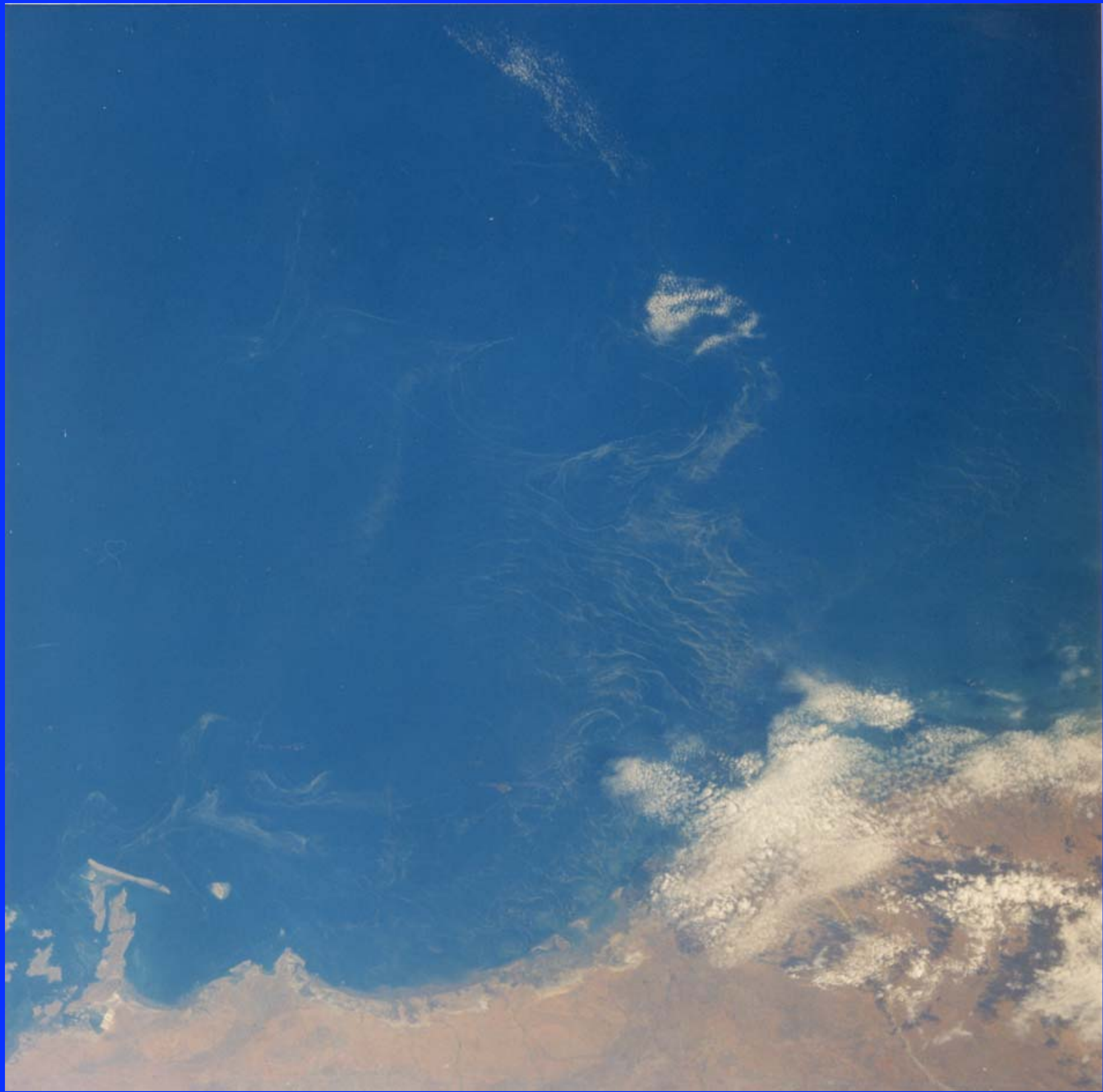

Satellite Image - *Trichodesmium* 14 July 1998

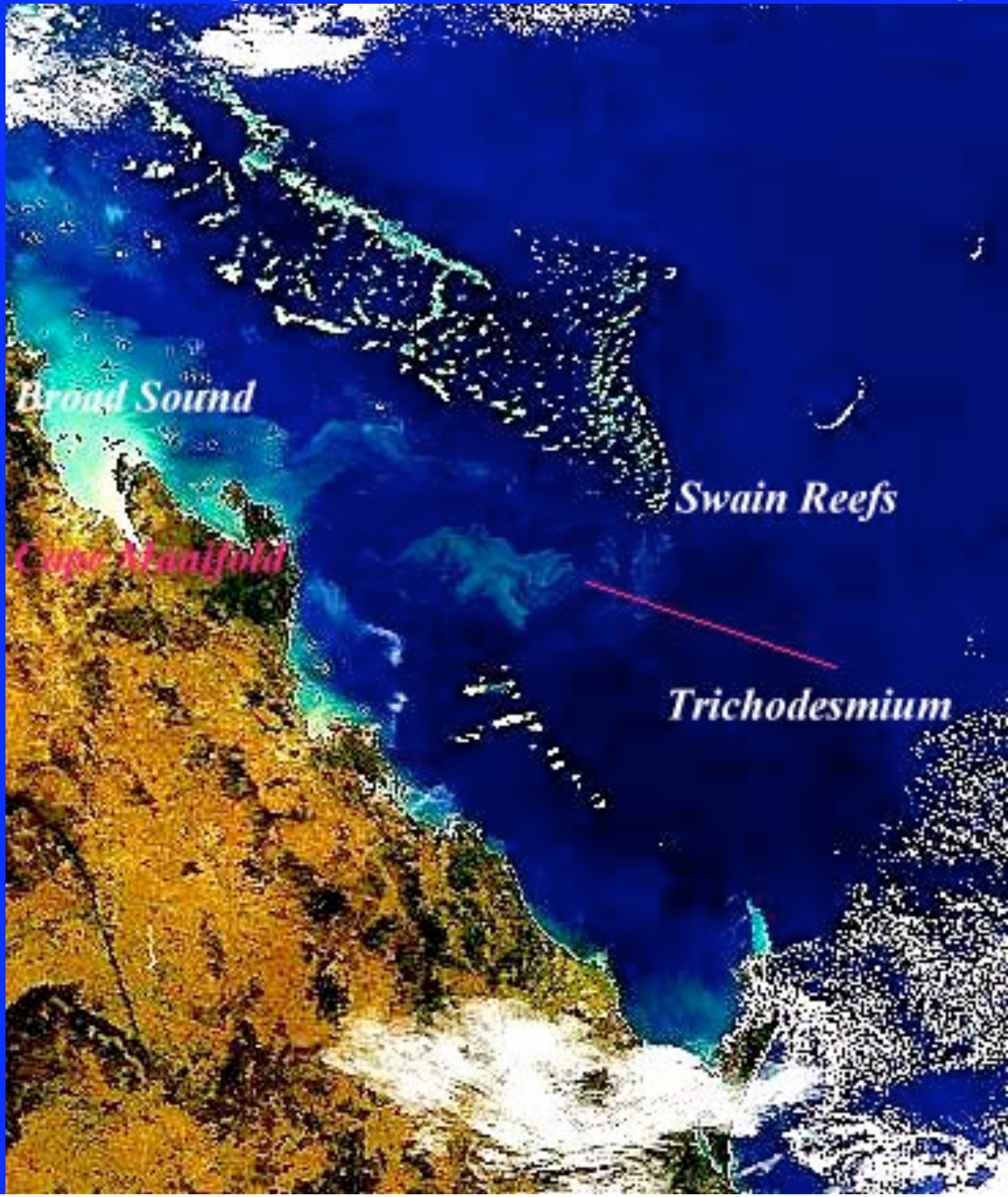


Earth at Night
More information available at:
http://antwrp.gsfc.nasa.gov/apod/ap001127.html
Astronomy Picture of the Day
2000 November 27
http://antwrp.gsfc.nasa.gov/apod/astropix.html

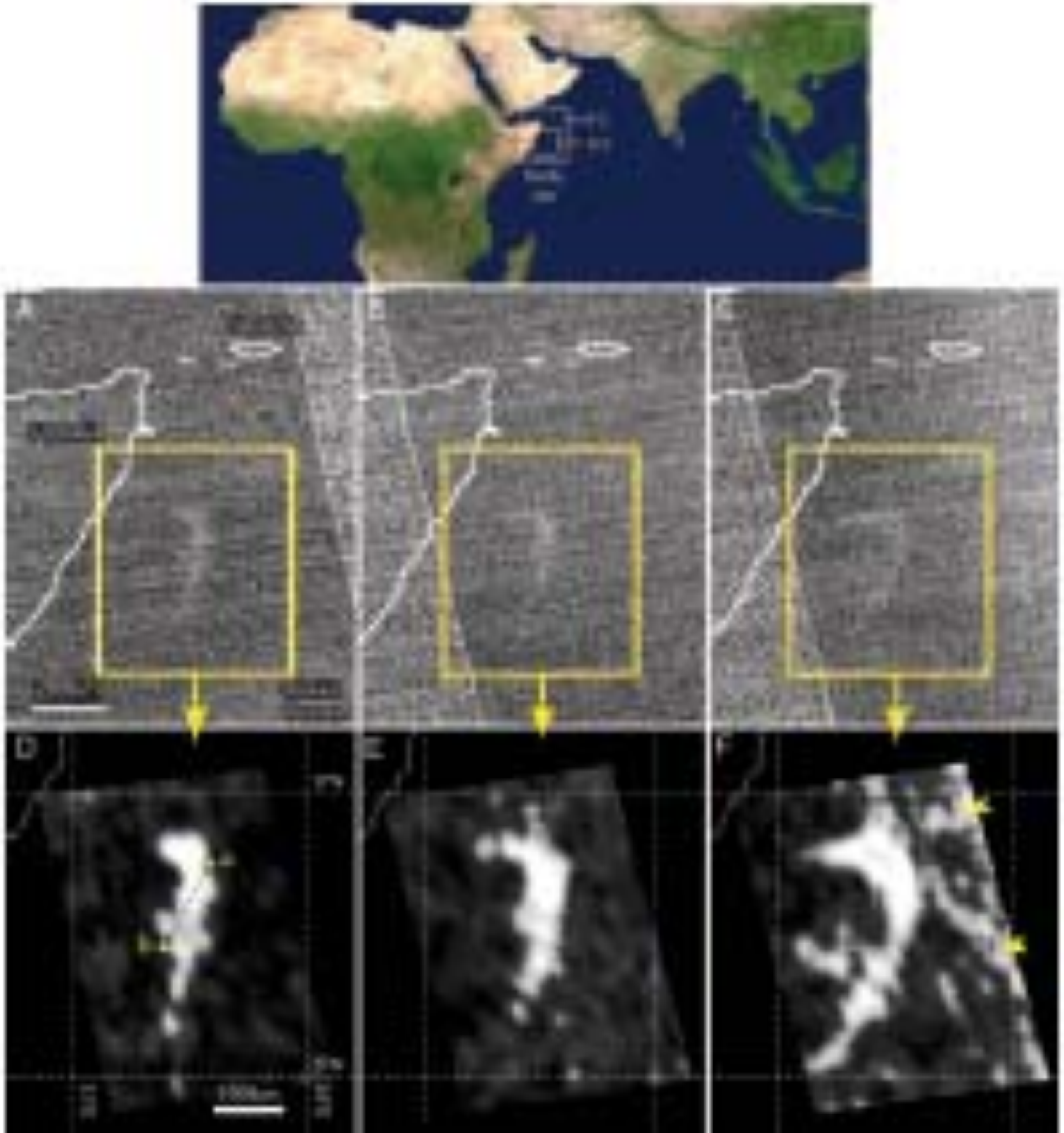

"The 27th of January, at the entrance of the vast Bay of Bengal …, about seven o'clock in the evening, the Nautilus … was sailing in a sea of milk …. Was it the effect of the lunar rays? No: for the moon … was lying hidden under the horizon … The whole sky, though lit by the sidereal rays, seemed black by contrast with the whiteness of the waters.

'It is called a milk sea', I explained …

'But sir, … can you tell me what causes such an effect? For I suppose the water is not really turned into milk.'

'No, my boy: and the whiteness which surprises you is caused only by the presence of myriads of infusoria, a sort of luminous little worm, gelatinous and without colour, of the thickness of a hair whose length is not more than seven-thousands of an inch. These insects adhere to one another sometimes for several leagues'

'… and you need not try to compute the number of these infusoria. You will not be able, for … ships have floated on these milk seas for more than forty miles'.

From Jules Verne Twenty Thousand Leagues Under the Sea – Indian Ocean, January 24th.

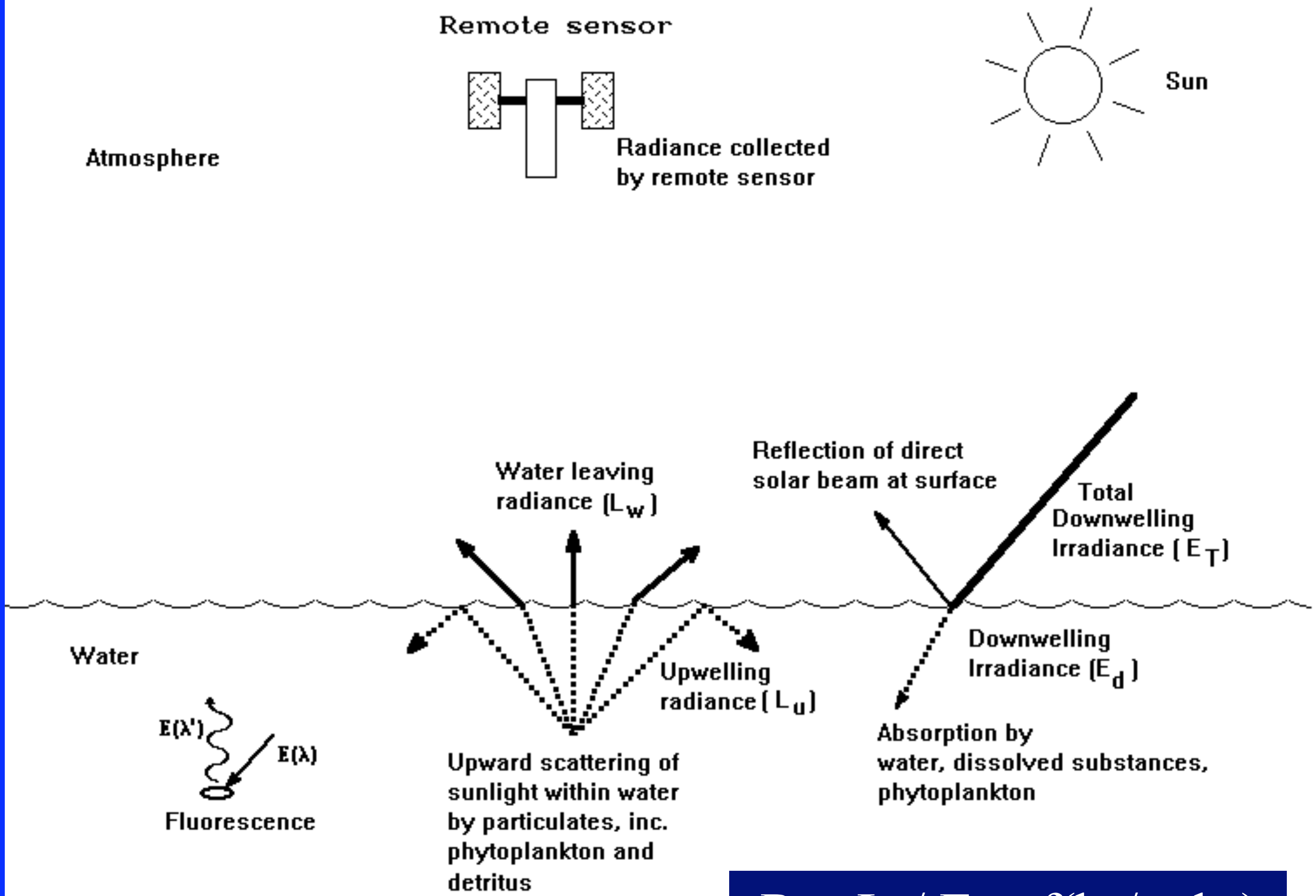

$$R_{rs}=L_u/\,E_d=f(b_b/a+b_b)$$

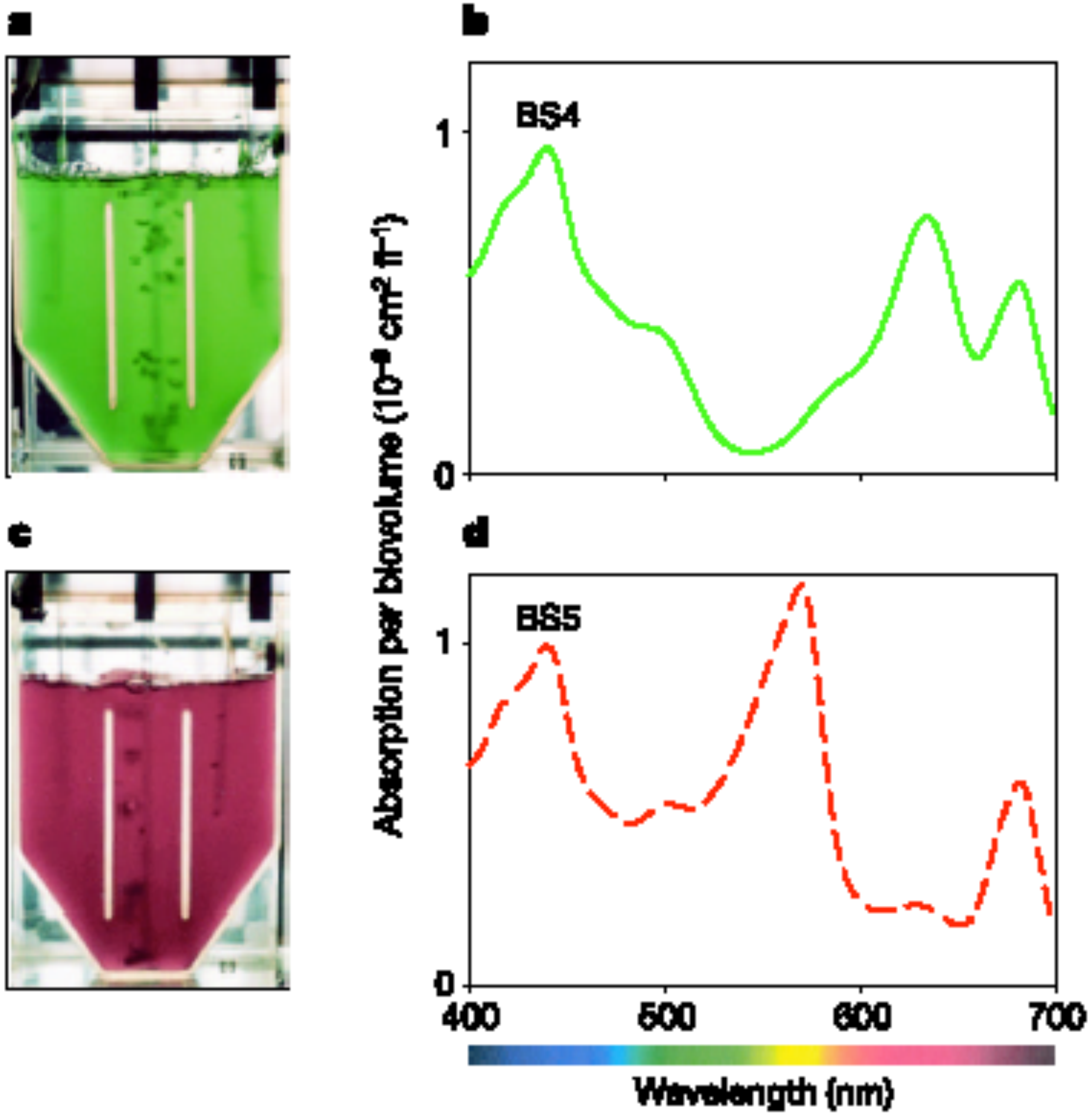

Figure 1 Optical characteristics of the picocyanobacteria BS4 and BS5. Monocultures of BS4 (**a**) and BS5 (**c**) grown in chemostats, and the light absorption spectra of BS4 (**b**) and BS5 (**d**).

From Stomp et al Nature 2004

FORWARD AND INVERSE SEMI-ANALYTICAL OCEAN COLOR MODELS

Forward models:

Generate R or Lw from Chl and/or IOPs

Chl, a, b_b → R(λ) or Lw(λ)

- Forward models can be useful to test if specific situations result in different Lw or reflectance spectra.

Inverse models:

Generate Chl and/or IOPs from R or Lw

R(λ) or Lw(λ) → Chl, a, b_b,…

From Stephane Maritorena

FORWARD AND INVERSE SEMI-ANALYTICAL OCEAN COLOR MODELS

Ocean color is very simple:

1) $a + b = c$ (IOPs)

2) $R \propto \dfrac{b_b}{a + b_b}$ (AOPs = f[IOPs]) From radiative transfer models

3) $a = f(R_1/R_2)$ Inverse model

From Stephane Maritorena

Ok, ok, it's not always that simple !

The R_{rs} to b_b/a relationship exists in various flavors

$$R_{rs} = \frac{t}{n_w^2} \frac{f}{Q} \left(\frac{b_b}{a + b_b} \right)$$

Water-air transmission term

"Geometry" factor

Can be reasonably well estimated based on viewing and illumination geometry, wind speed and salinity

From Stephane Maritorena

It's not always that simple and most terms have their own spectral dependence

$$R_{rs}(\lambda) = \frac{t}{n_w^2}\frac{f(\lambda)}{Q(\lambda)}\left[\frac{\underline{b_{bw}}(\lambda) + b_{bp}(\lambda)}{\underline{a_w}(\lambda) + a_\varphi(\lambda) + a_d(\lambda) + a_g(\lambda) + \underline{b_{bw}}(\lambda) + b_{bp}(\lambda)}\right]$$

- Reflection by bright shallow bottom was not considered here.
- Various ways exist to fill the right-end side of the equation and get a forward model.
- Optical properties of water is fixed and assumed to be well known

Tricky part:

parameterization of b_{bp} and non-water absorption terms.
Their relative variations need to be realistic

From Stephane Maritorena

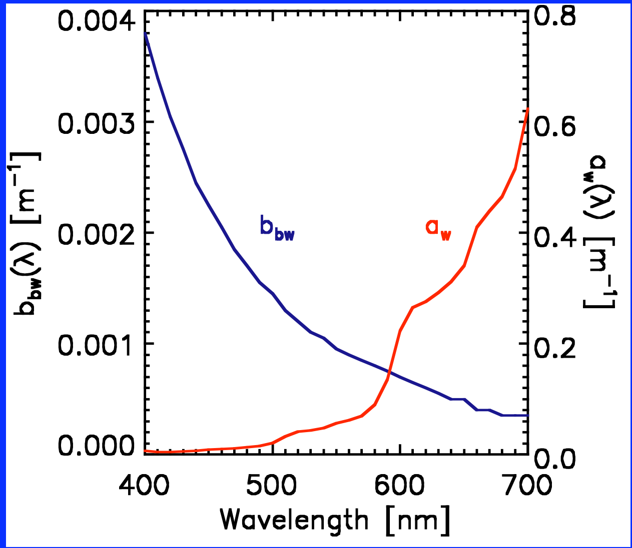

From Stephane Maritorena

Particulate backscattering, b_{bp}

$$b_p(550) = 0.416\ \text{chl}^{\,0.766}$$

$$b_{bp}(\lambda) = \{0.002 + 0.01[0.5 - 0.25\ \log_{10}[\text{chl}]]\ (\lambda/550)^{\nu}\}\ b_p(550)$$

$$\nu = 0.5\ (\log_{10}[\text{chl}] - 0.3)\ \text{and}\ \nu = 0\ \text{when}\ [\text{chl}] > 2\ \text{mg m}^{-3}$$

(Morel, 1988; Morel & Maritorena, 2001)

$$b_{bp}(\lambda) = b_{bp}(\lambda_0)(\lambda/\lambda_0)^{\nu}$$

$$b_{bp}(\lambda_0) = f(\text{chl})\ \text{and}\ \nu = f(b_{bp}(\lambda_0))$$

(Reynolds et al., 2001)

$$b_{bp}(\lambda) = \underbrace{0.039\ b_{ps}{}^{o}(\lambda)\ P_s}_{\text{Small particles}} + \underbrace{0.00064\ b_{pl}{}^{o}(\lambda)\ P_l}_{\text{Large particles}}$$

(Haltrin & Kattawar, 1991)

$$b_b = b_{bw} + b_{b\varphi 1} + b_{b\varphi 2} + \ldots + b_{b\varphi n} + b_{bdet} + b_{bmin} + b_{bbub}$$

(Stramski et al., 2001)

$$b_{bp}(\lambda) = \tilde{b}_{bp}\ [c_p(\lambda) - a_p(\lambda)]$$

(Roesler & Boss, 2003)

Other parameterizations of b_{bp} exist (H. Loisel, Z. Lee, …)

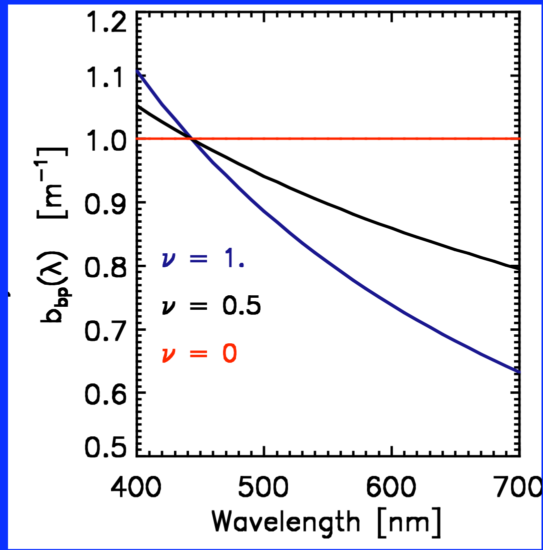

From Stephane Maritorena

$$R_{rs}(\lambda) = \frac{t}{n_w^{\ 2}} \frac{f(\lambda)}{Q(\lambda)} \left[\frac{b_{bw}(\lambda) + b_{bp}(\lambda)}{a_w(\lambda) + a_\varphi(\lambda) + a_d(\lambda) + a_g(\lambda) + b_{bw}(\lambda) + b_{bp}(\lambda)} \right]$$

Absorption

Phytoplankton $a_\varphi(\lambda) = A(\lambda)chl^{B(\lambda)}$

From Stephane Maritorena

Absorption $a = a_w + a_{\varphi 1} + a_{\varphi 2} + \ldots + a_{\varphi n} + a_{det} + a_{min} + a_y$

Phytoplankton $a_\varphi(\lambda) = A(\lambda)chl^{B(\lambda)}$

Detritus $a_d(\lambda) = a_d(\lambda_0) \exp[S_d (\lambda_0 - \lambda)]$

Dissolved organic matter $a_y(\lambda) = a_y(\lambda_0) \exp[S_y (\lambda_0 - \lambda)]$

From Stephane Maritorena

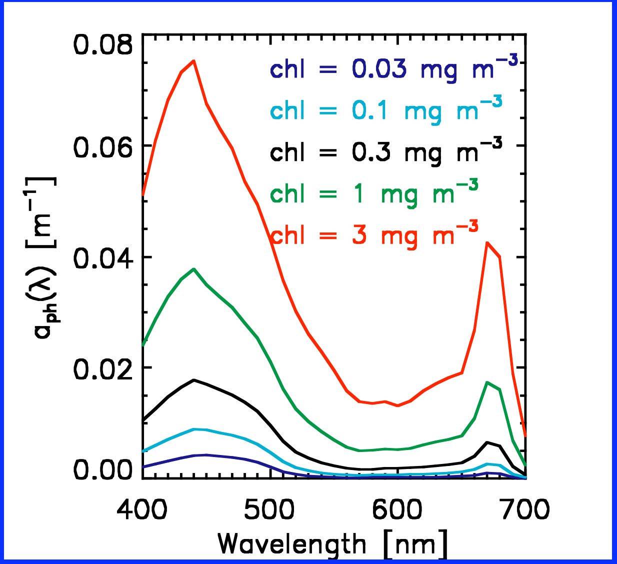

0.08
0.06
0.04
0.02
0.00
400
500
600
700
Wavelength [nm]
$a_{ph}(\lambda)$ [m^{-1}]
chl = 0.03 mg m^{-3}
chl = 0.1 mg m^{-3}
chl = 0.3 mg m^{-3}
chl = 1 mg m^{-3}
chl = 3 mg m^{-3}

$$R_{rs}(\lambda) = \frac{t}{n_w^{\ 2}} \frac{f(\lambda)}{Q(\lambda)} \left[\frac{b_{bw}(\lambda) + b_{bp}(\lambda)}{a_w(\lambda) + a_\varphi(\lambda) + \underline{a_d(\lambda)} + \underline{a_g(\lambda)} + b_{bw}(\lambda) + b_{bp}(\lambda)} \right]$$

Absorption

Detritus $a_d(\lambda) = a_d(\lambda_0) \exp[S_d (\lambda_0 - \lambda)]$

Dissolved organic matter $a_g(\lambda) = a_g(\lambda_0) \exp[S_g (\lambda_0 - \lambda)]$

From Stephane Maritorena

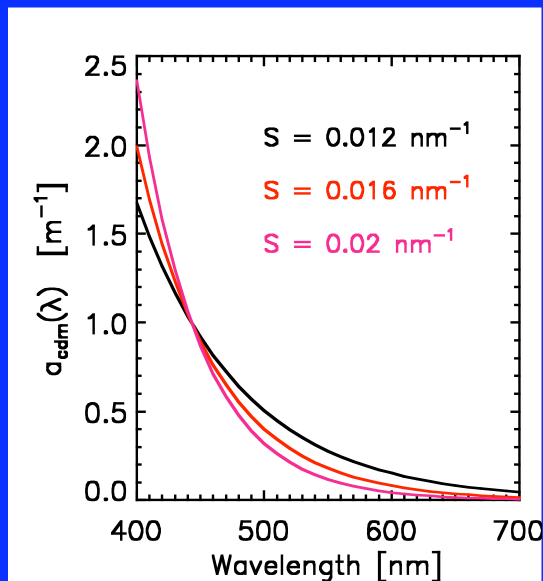

From Stephane Maritorena

FORWARD SEMI-ANALYTICAL OCEAN COLOR MODELS

Putting all together,

$$R_{rs}(\lambda) = \frac{t}{n_w^{2}} \frac{f(\lambda)}{Q(\lambda)} \left(\frac{b_{bw}(\lambda) + b_{bp}(\lambda)}{a_w(\lambda) + a_{\varphi}(\lambda) + a_d(\lambda) + a_g(\lambda) + b_{bw}(\lambda) + b_{bp}(\lambda)} \right)$$

From Stephane Maritorena

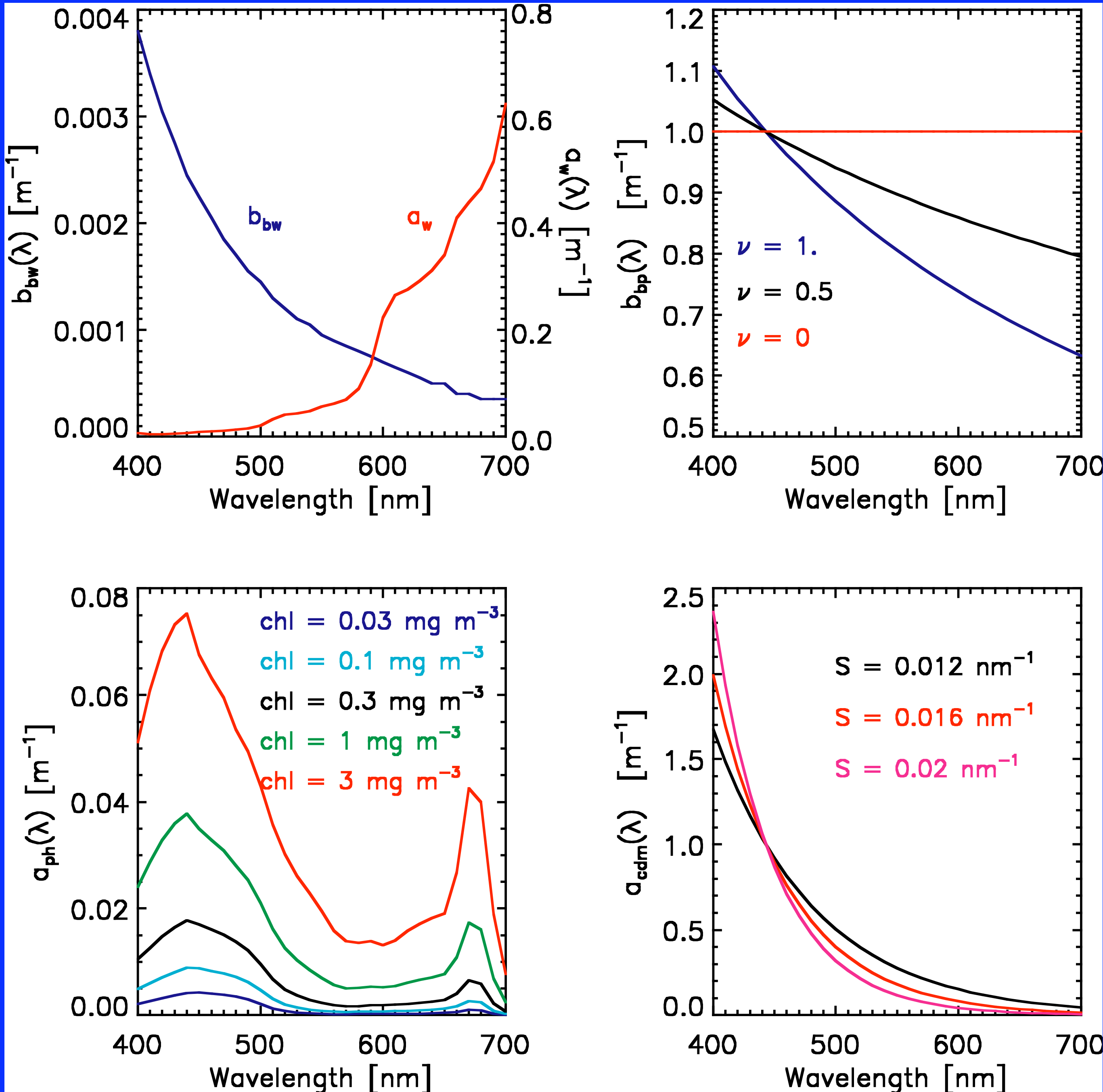

0.004
0.003
0.002
0.001
0.000
0.8
0.6
0.4
0.2
0.0
$b_{bw}(\lambda)$ [m^{-1}]
$a_w(\lambda)$ [m^{-1}]
b_{bw}
a_w
400
500
600
700
Wavelength [nm]
1.2
1.1
1.0
0.9
0.8
0.7
0.6
0.5
$b_{bp}(\lambda)$ [m^{-1}]
ν = 1.
ν = 0.5
ν = 0
400
500
600
700
Wavelength [nm]
0.08
0.06
0.04
0.02
0.00
$a_{ph}(\lambda)$ [m^{-1}]
chl = 0.03 mg m^{-3}
chl = 0.1 mg m^{-3}
chl = 0.3 mg m^{-3}
chl = 1 mg m^{-3}
chl = 3 mg m^{-3}
400
500
600
700
Wavelength [nm]
2.5
2.0
1.5
1.0
0.5
0.0
$a_{cdm}(\lambda)$ [m^{-1}]
S = 0.012 nm^{-1}
S = 0.016 nm^{-1}
S = 0.02 nm^{-1}
400
500
600
700
Wavelength [nm]

"Historical" forward models (Gordon et al., 1988; Morel, 1988) are chlorophyll-based: Chl → R (λ)

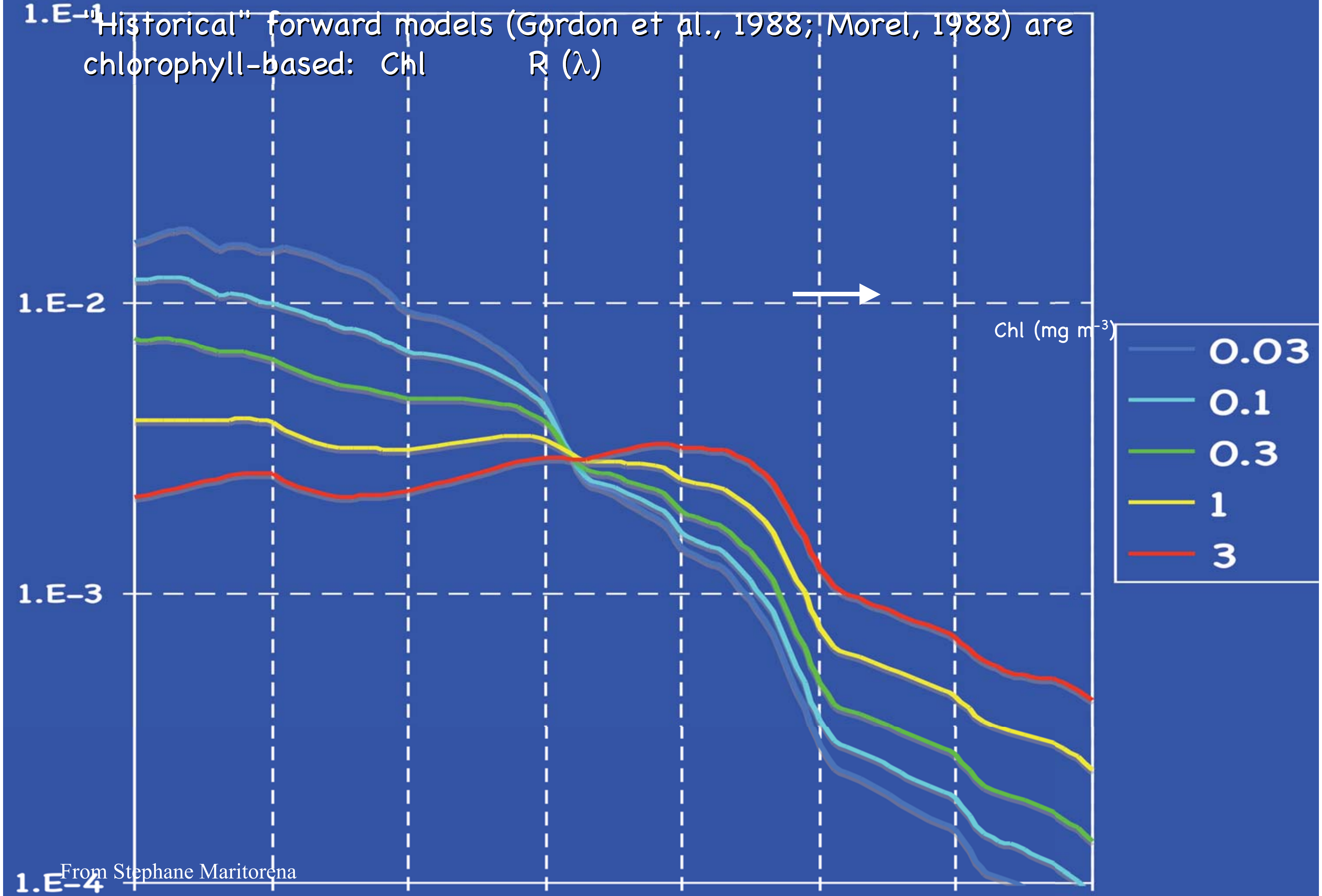

From Stephane Maritorena

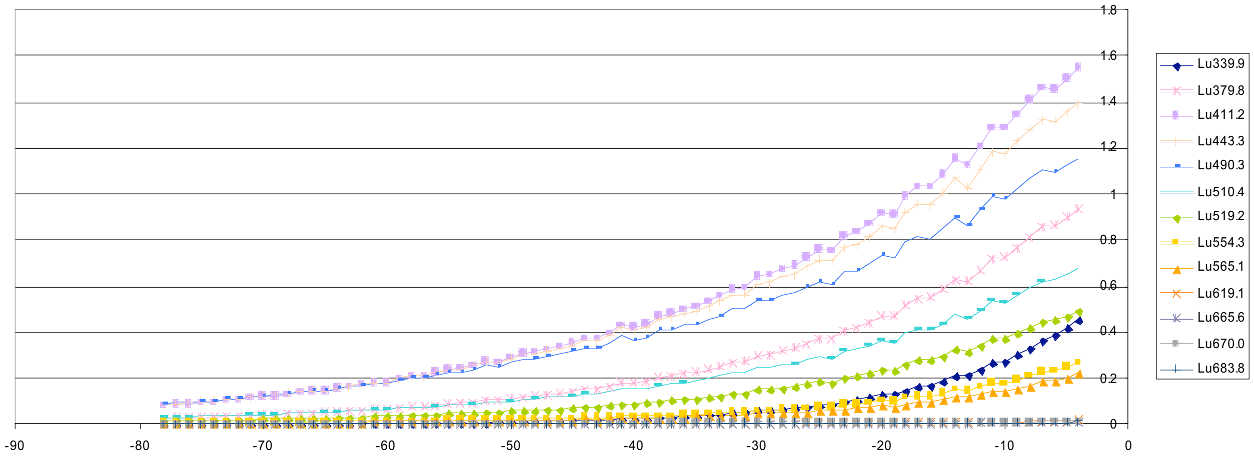

1.8
1.6
1.4
1.2
1
0.8
0.6
0.4
0.2
0
-90
-80
-70
-60
-50
-40
-30
-20
-10
0
Lu339.9
Lu379.8
Lu411.2
Lu443.3
Lu490.3
Lu510.4
Lu519.2
Lu554.3
Lu565.1
Lu619.1
Lu665.6
Lu670.0
Lu683.8

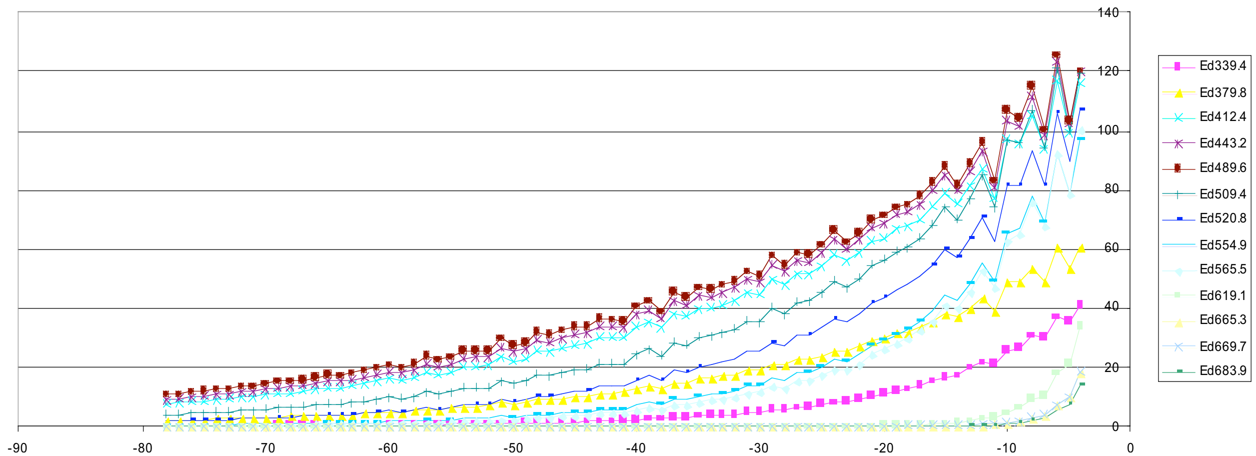

140
120
100
80
60
40
20
0
-90
-80
-70
-60
-50
-40
-30
-20
-10
0
Ed339.4
Ed379.8
Ed412.4
Ed443.2
Ed489.6
Ed509.4
Ed520.8
Ed554.9
Ed565.5
Ed619.1
Ed665.3
Ed669.7
Ed683.9

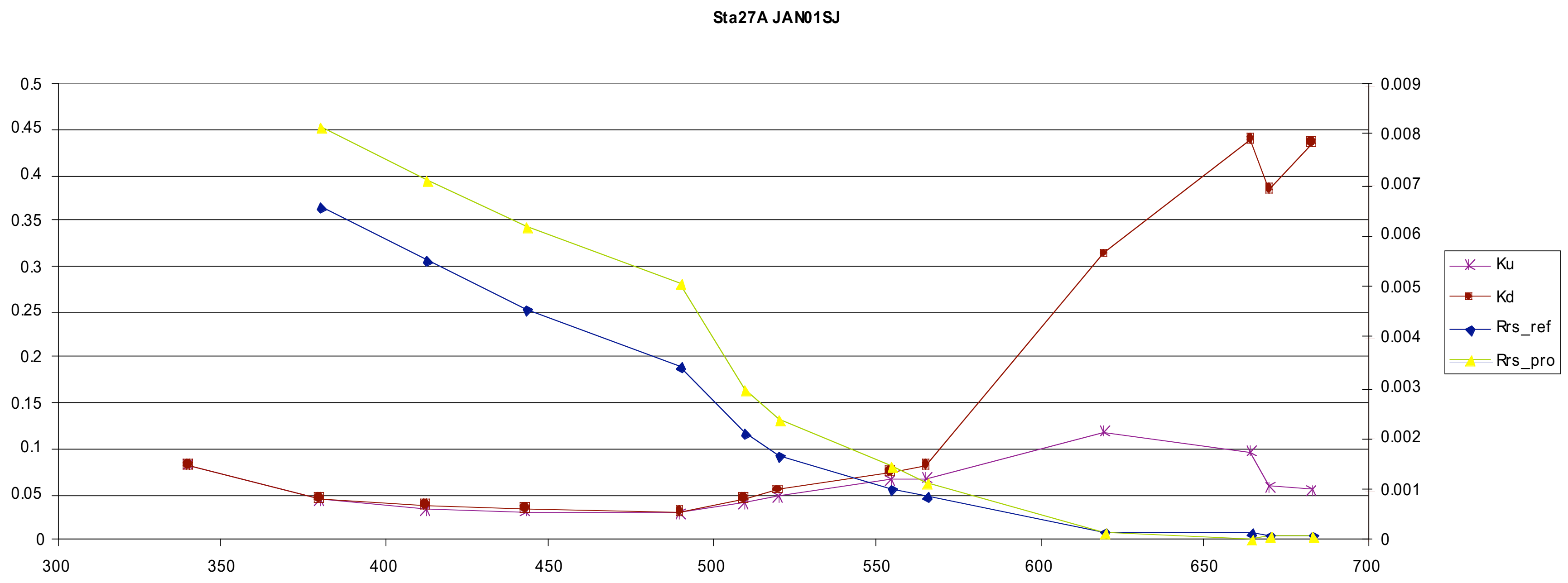

Sta27A JAN01SJ
0.5
0.45
0.4
0.35
0.3
0.25
0.2
0.15
0.1
0.05
0
0.009
0.008
0.007
0.006
0.005
0.004
0.003
0.002
0.001
0
300
350
400
450
500
550
600
650
700
Ku
Kd
Rrs_ref
Rrs_pro

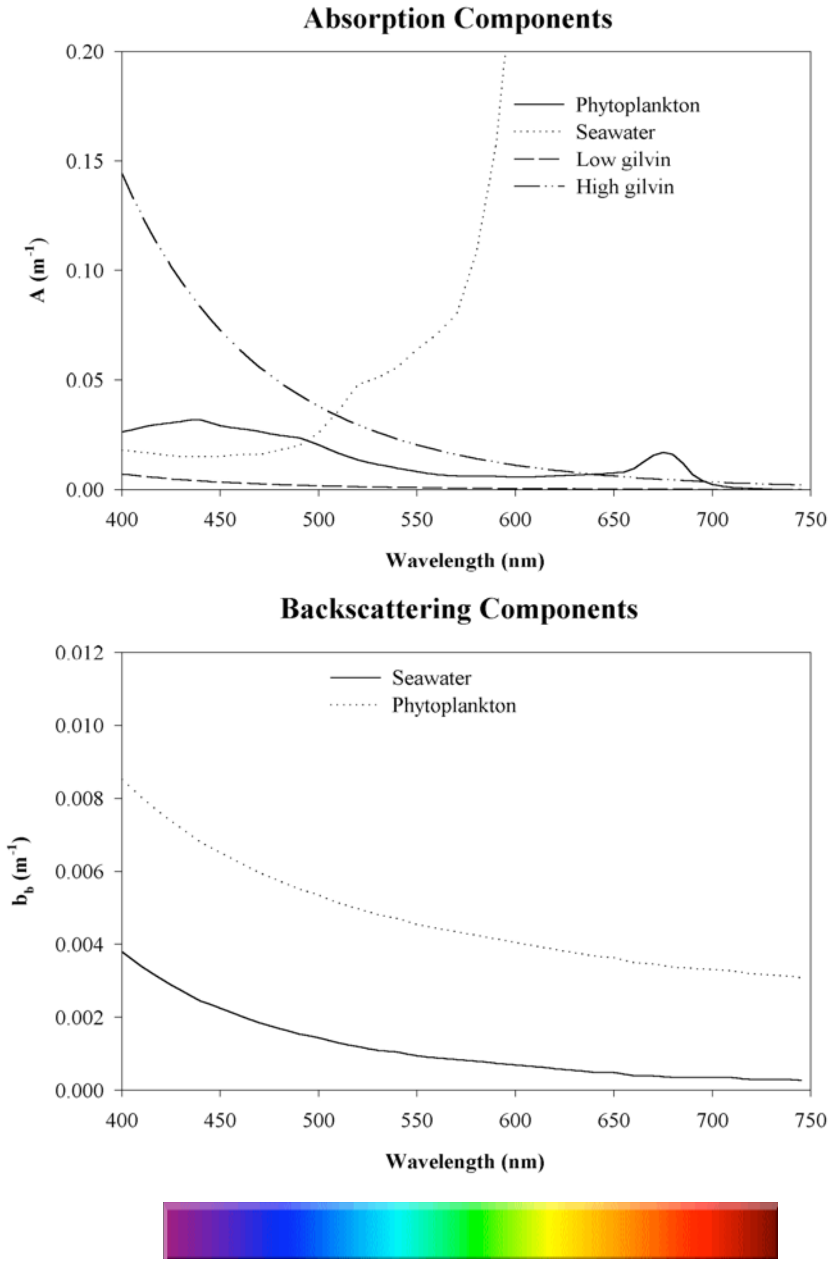

Absorption Components
Phytoplankton
Seawater
Low gilvin
High gilvin
A (m-1)
0.20
0.15
0.10
0.05
0.00
400
450
500
550
600
650
700
750
Wavelength (nm)
Backscattering Components
Seawater
Phytoplankton
bb (m-1)
0.012
0.010
0.008
0.006
0.004
0.002
0.000
400
450
500
550
600
650
700
750
Wavelength (nm)

Gaussian Curve Fit to *Trichodesmium*
Chlorophyll Specific Absorption

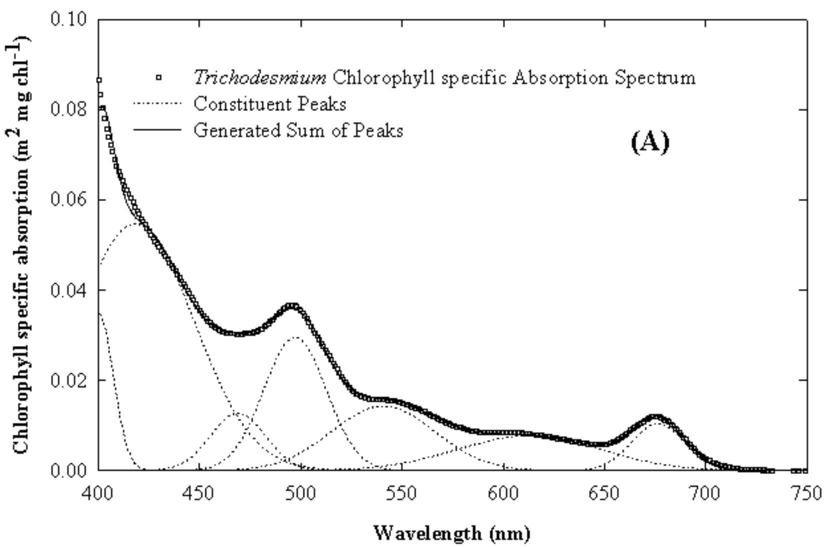

Extracted pigment absorption

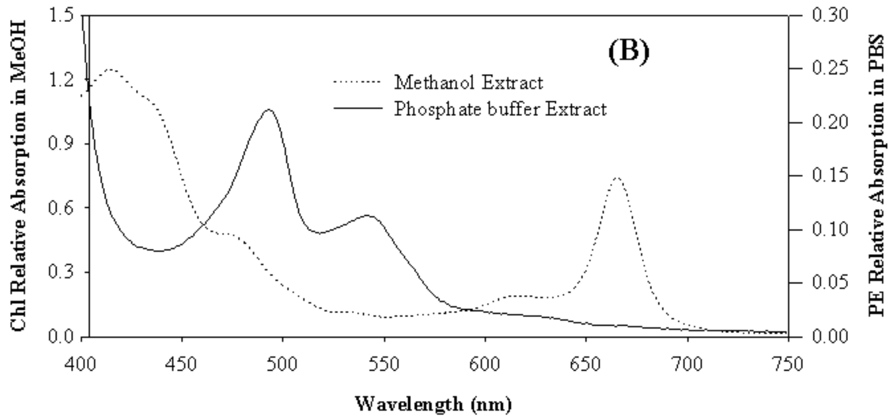

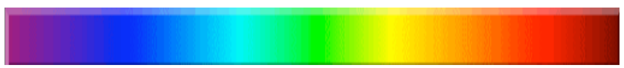

Reflectance model for Chl=0.1 mg/m^3

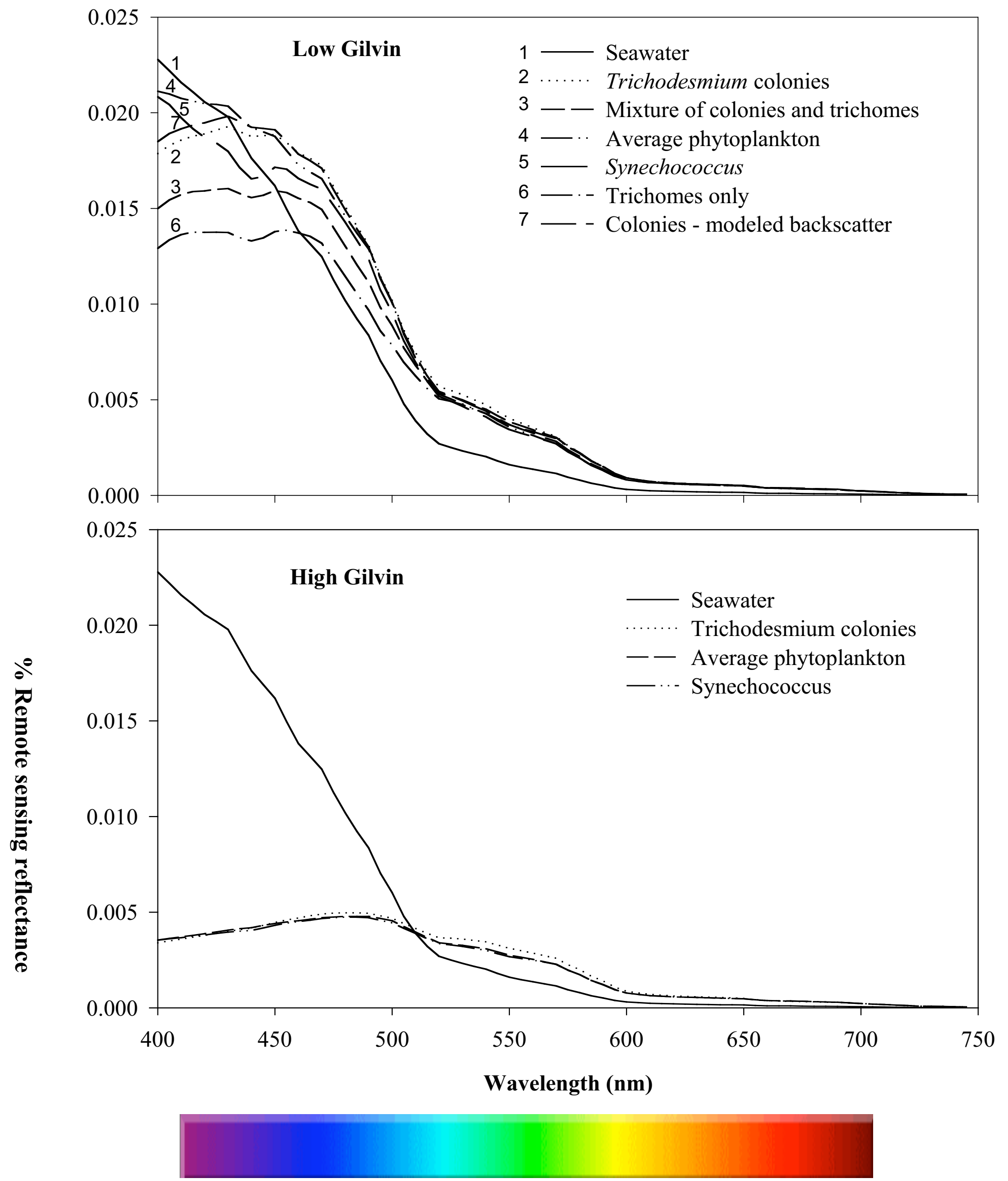

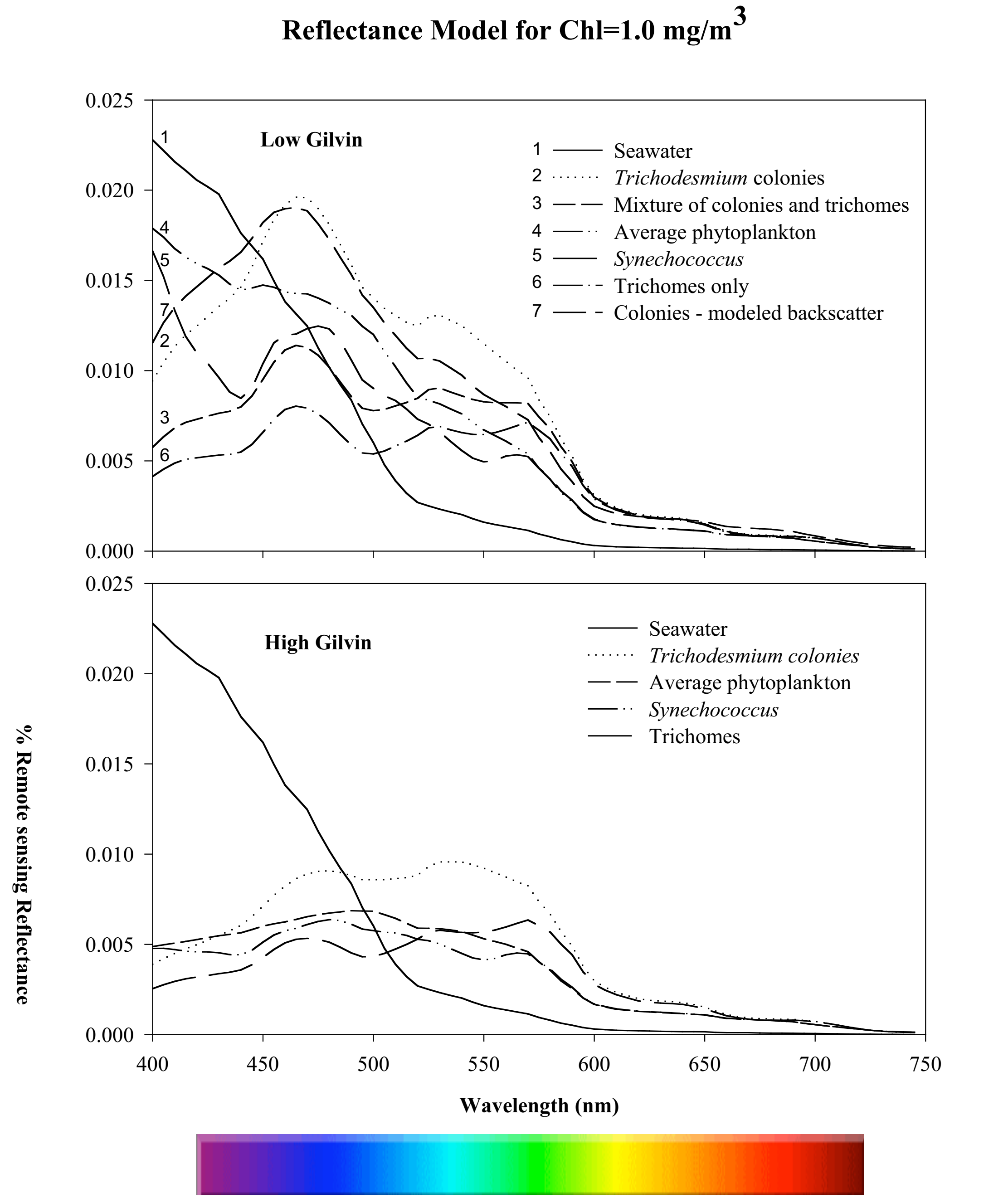

Reflectance Model for Chl=1.0 mg/m3
Low Gilvin
1 Seawater
2 Trichodesmium colonies
3 Mixture of colonies and trichomes
4 Average phytoplankton
5 Synechococcus
6 Trichomes only
7 Colonies - modeled backscatter
High Gilvin
Seawater
Trichodesmium colonies
Average phytoplankton
Synechococcus
Trichomes
% Remote sensing Reflectance
Wavelength (nm)
0.025
0.020
0.015
0.010
0.005
0.000
400
450
500
550
600
650
700
750

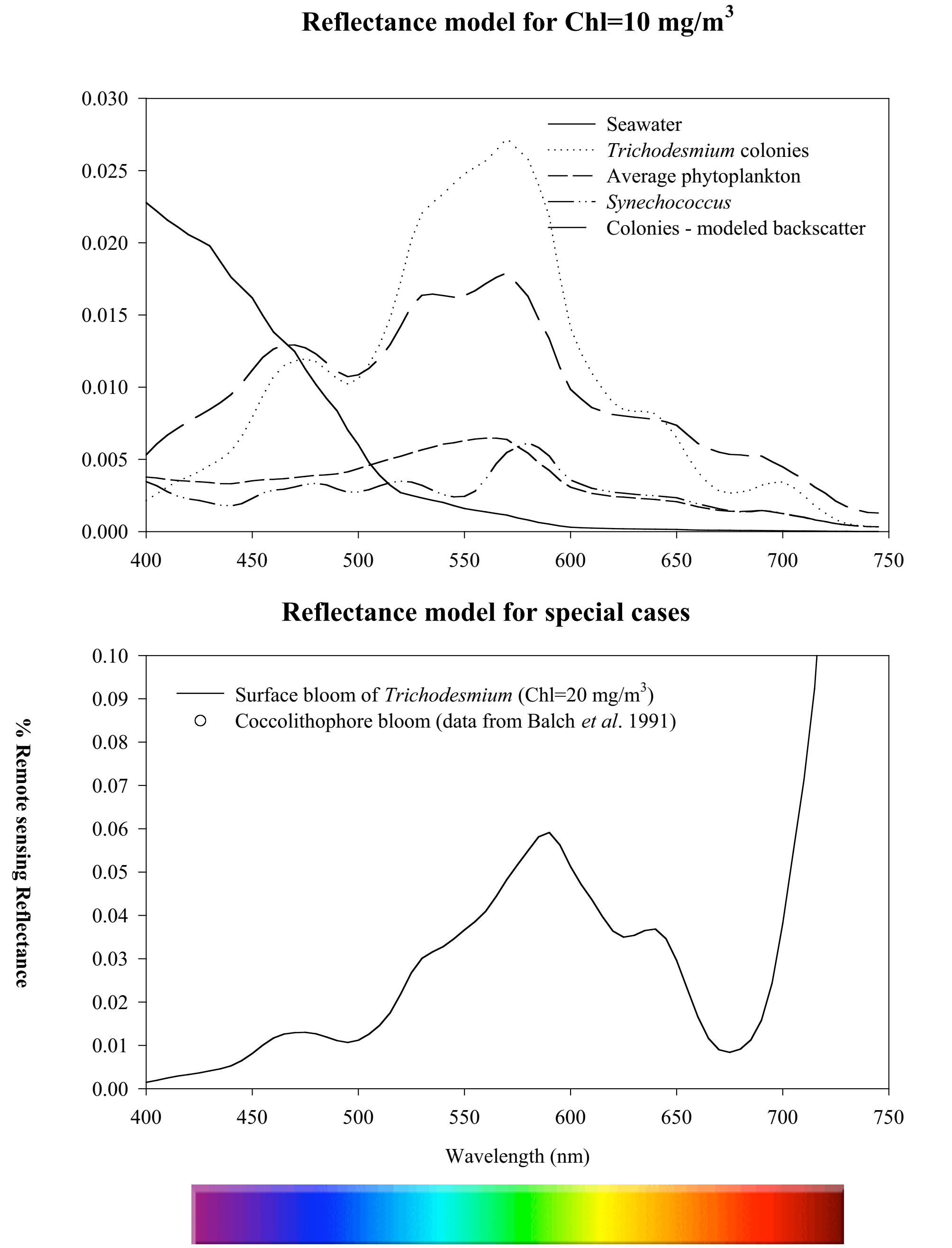

Reflectance model for Chl=10 mg/m3
Seawater
Trichodesmium colonies
Average phytoplankton
Synechococcus
Colonies - modeled backscatter
0.030
0.025
0.020
0.015
0.010
0.005
0.000
400
450
500
550
600
650
700
750
Reflectance model for special cases
Surface bloom of Trichodesmium (Chl=20 mg/m3)
Coccolithophore bloom (data from Balch et al. 1991)
% Remote sensing Reflectance
0.10
0.09
0.08
0.07
0.06
0.05
0.04
0.03
0.02
0.01
0.00
Wavelength (nm)

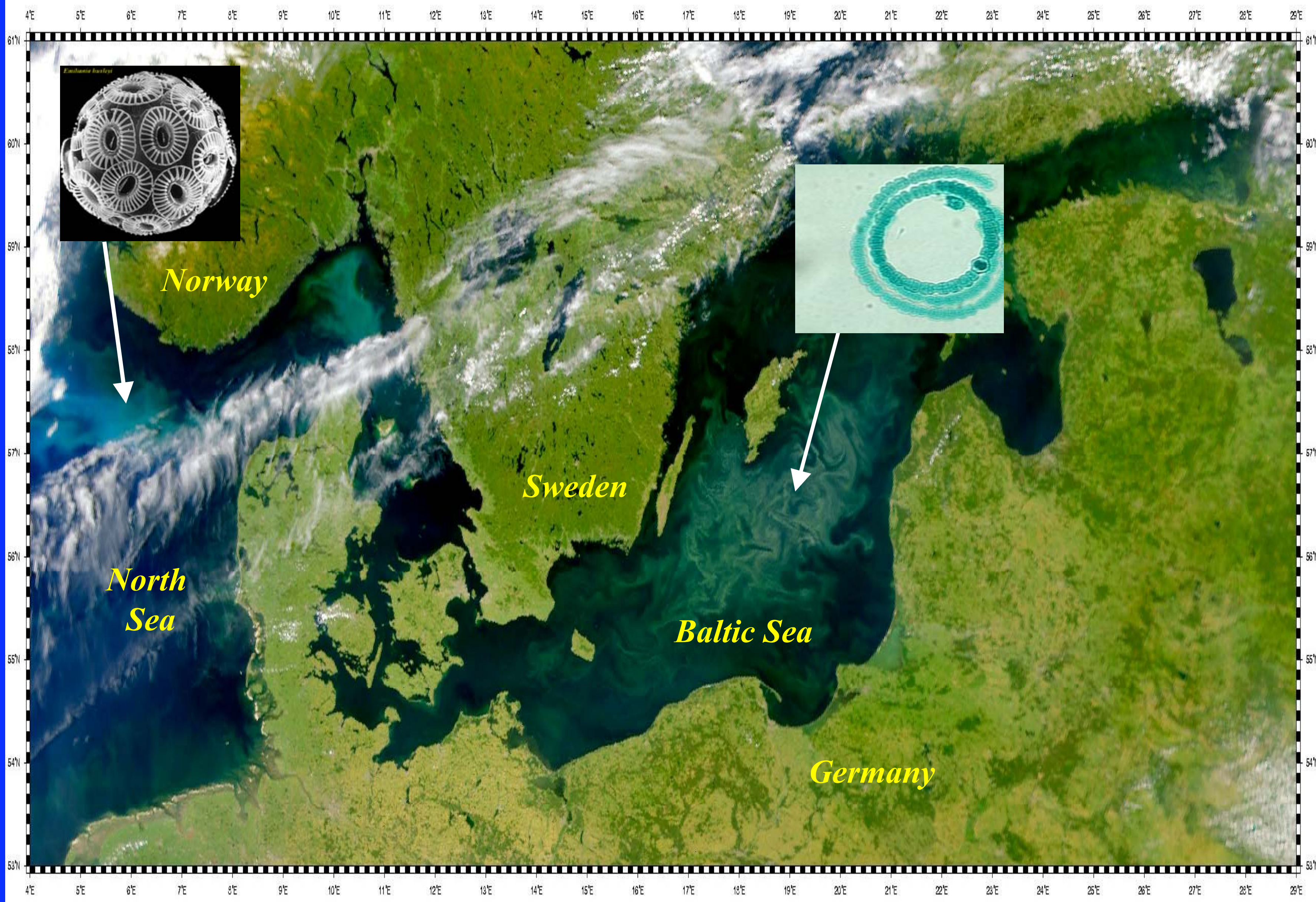
Norway
Sweden
North Sea
Baltic Sea
Germany


FOTO: KUSTBEVAKNINGSFLYGET

Synthetic Aperture RADAR

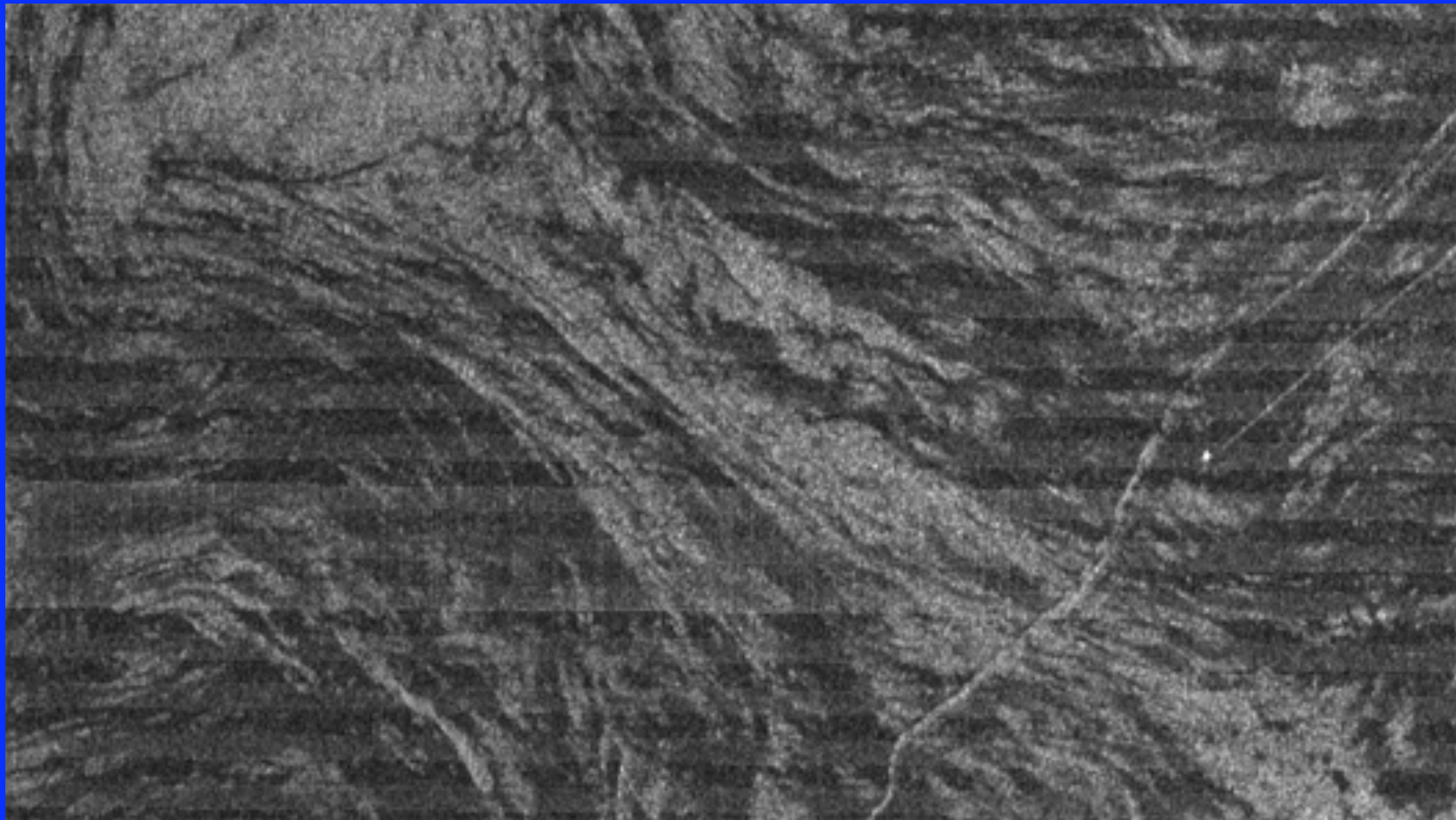

SAR Image from 3 August 1999

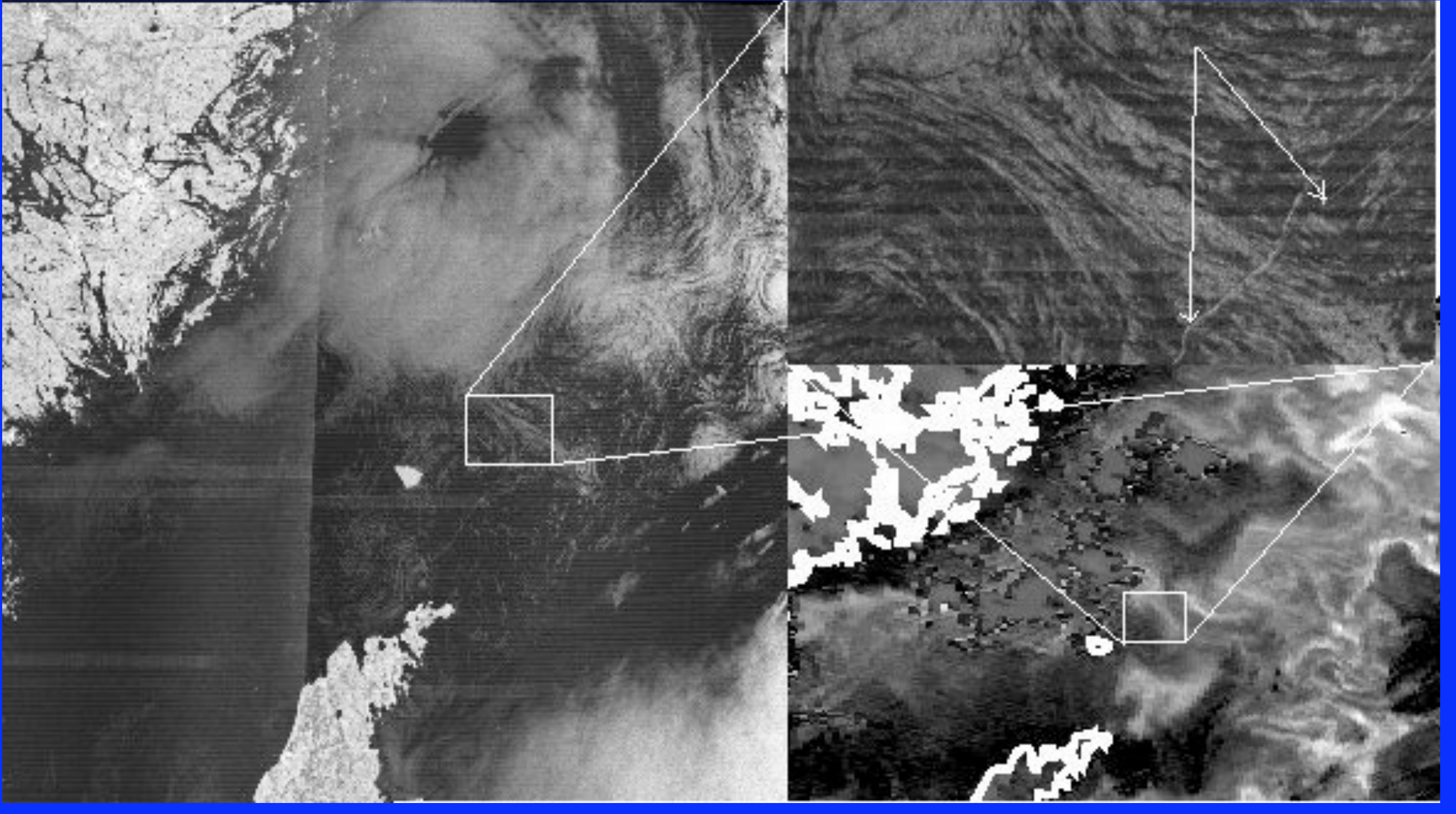

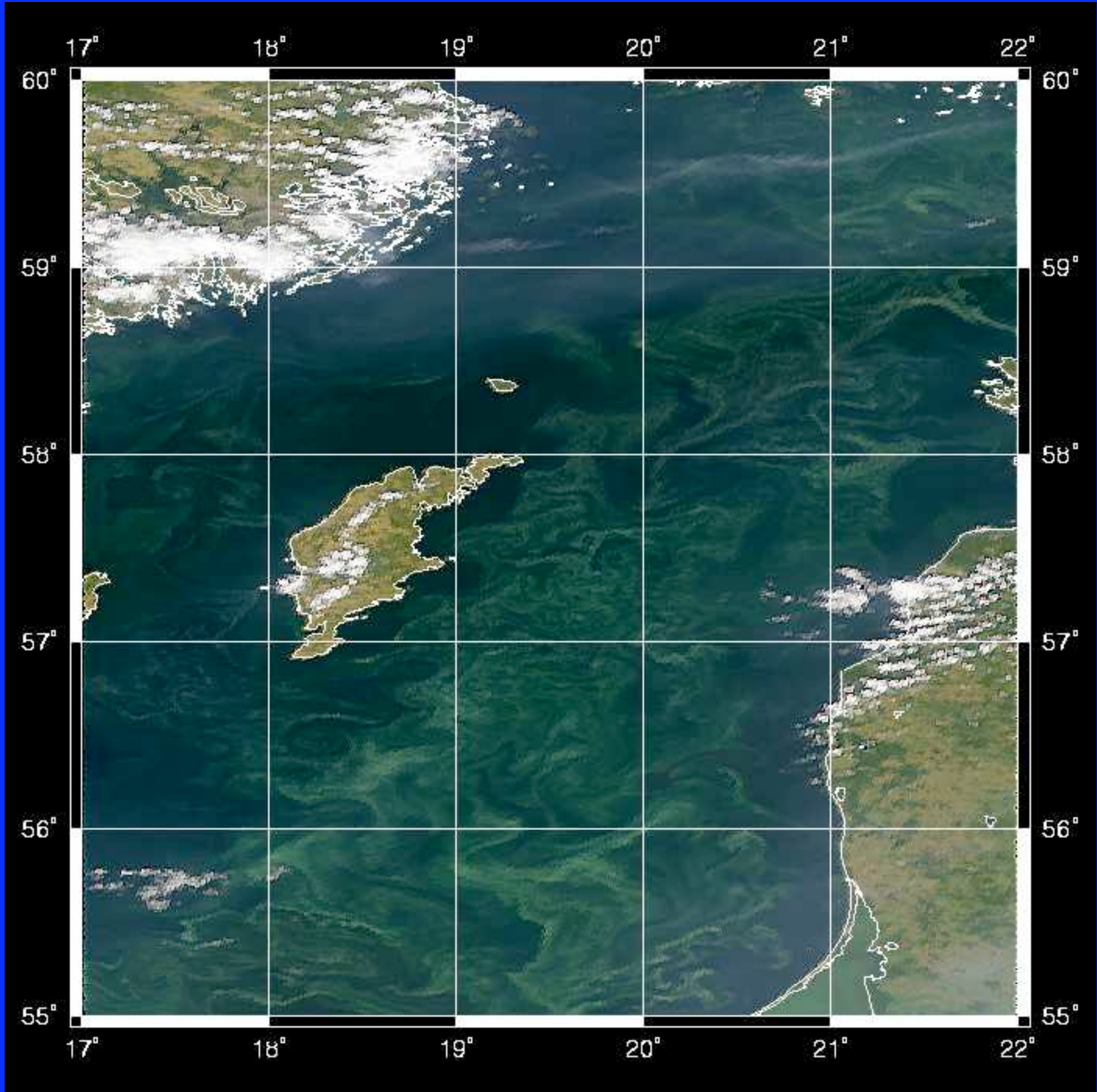
17°
18°
19°
20°
21°
22°
60°
59°
58°
57°
56°
55°

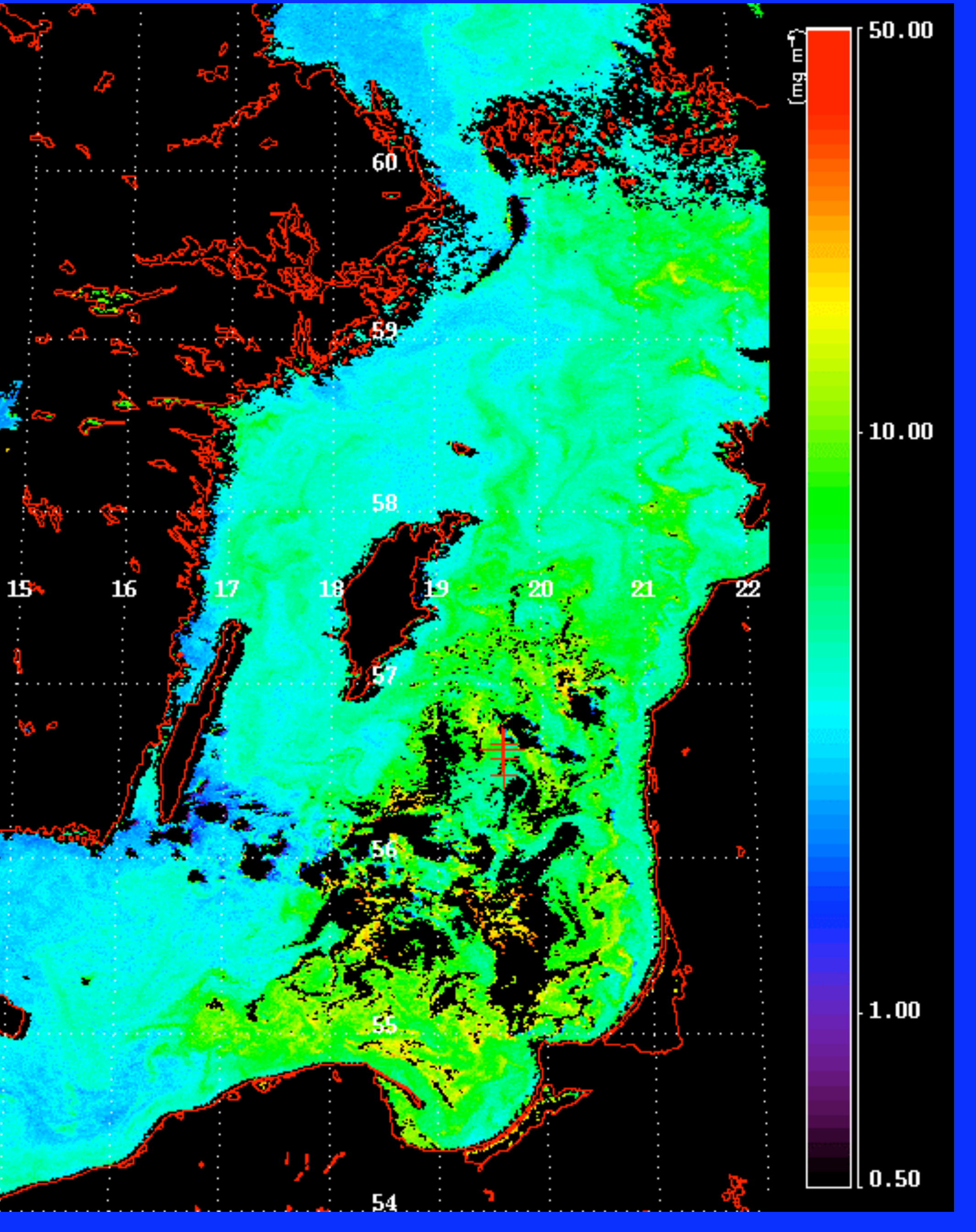

60
59
58
57
56
55
54
15
16
17
18
19
20
21
22
50.00
10.00
1.00
0.50

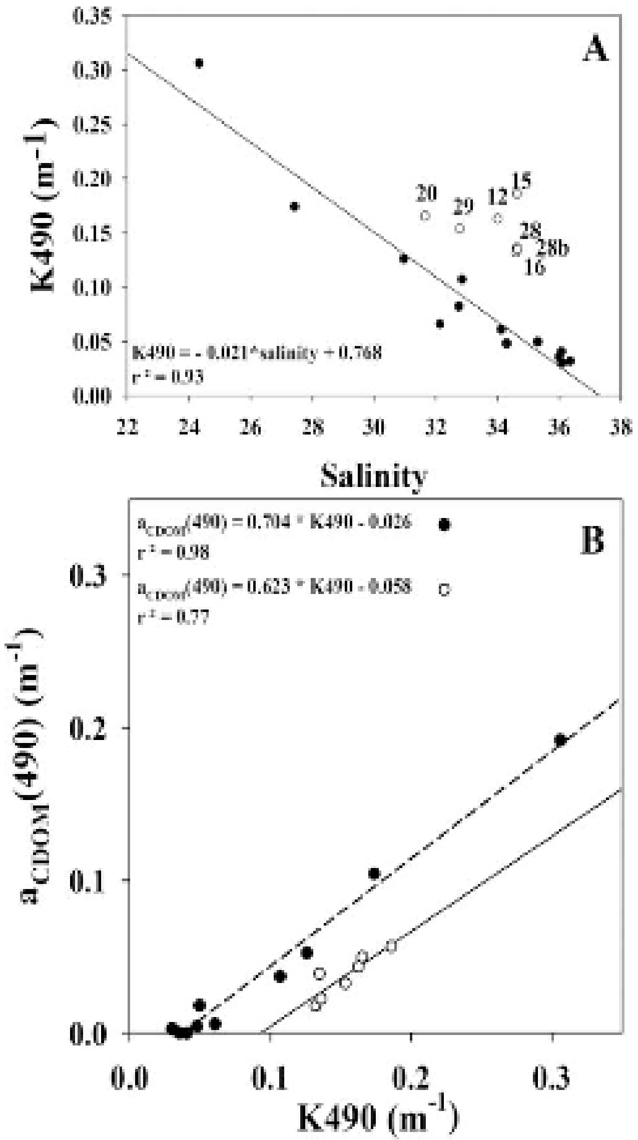

Figure 5. (a) K490 to salinity dependence and (b) $a_{CDOM}(490)$ to K490 dependence in the WTNA during May 2003. Solid circles represent the Amazon River plume (Transect A) and offshore waters (Region A and Region B without intense diatoms bloom). Open circles represent stations with intense diatoms bloom (Region B). Numbers refer to stations. Lines represent linear regressions with parameters reported in figure and statistics in Table 1.

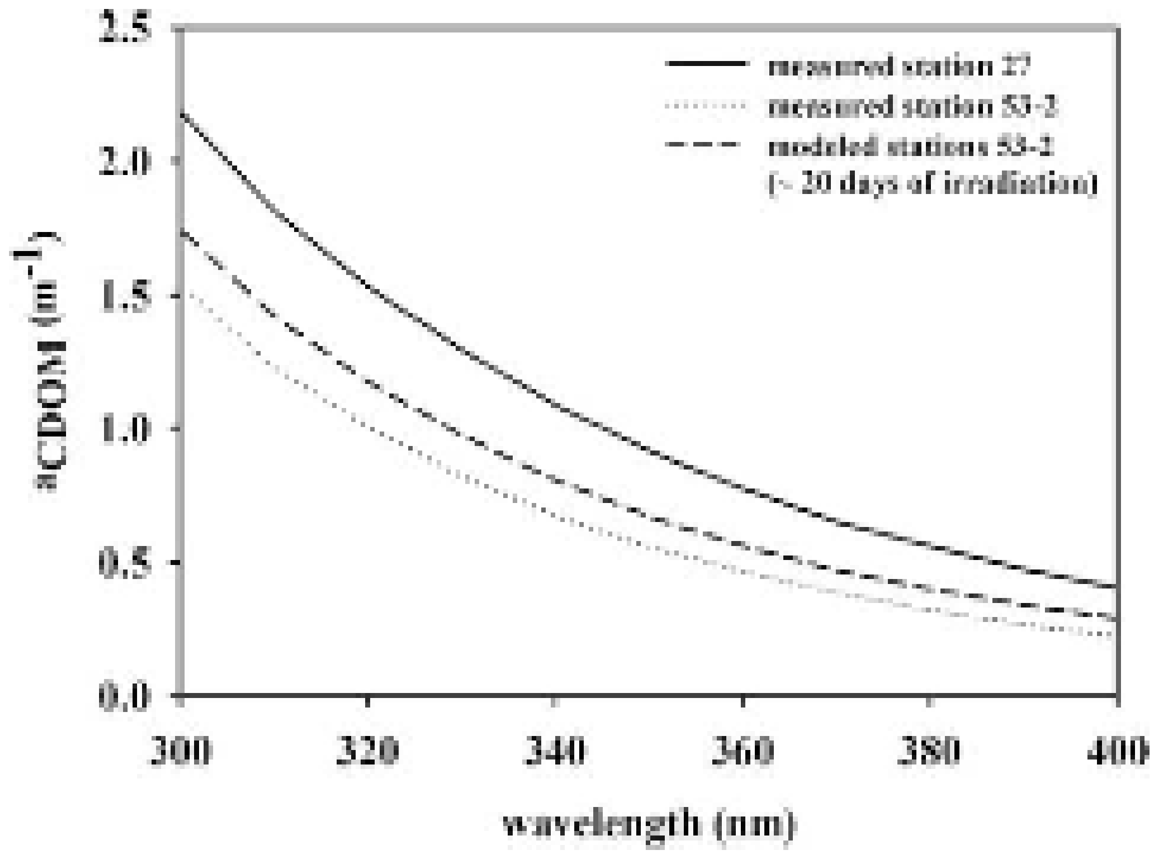

Figure 10. Measured (stations 27 and 53-2) and modeled (after 20 days of light exposure) a_{CDOM} during August 2001 in the WTNA.

Del Vecchio, R. and A. Subramaniam (2004) Influence of the Amazon River on the surface optical properties of the Western Tropical North Atlantic Ocean. Journal of Geophysical Research. 109, C11001, doi:10.1029/2004JC002503

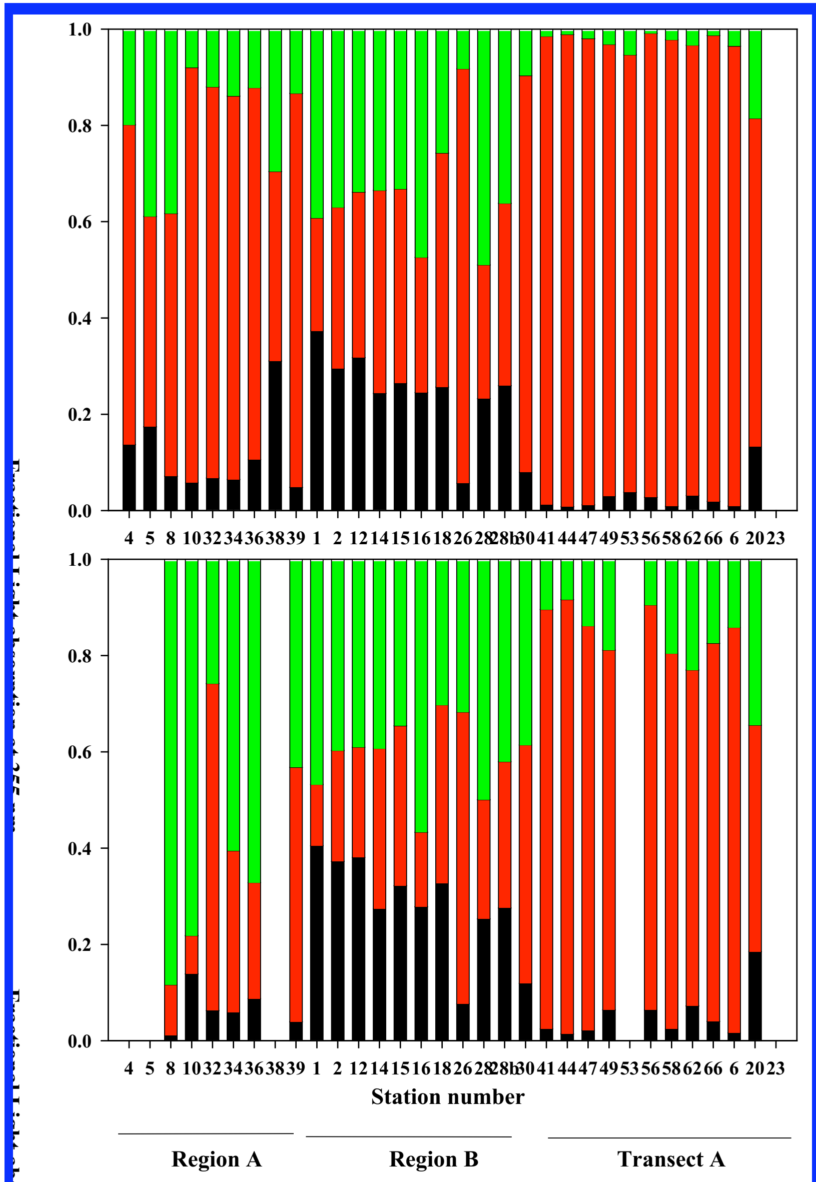

offshore out-of-plume   offshore in-plume closer to shore in-plume

CDOM absorption coefficient at 355 nm [a_{CDOM}(355)] (m^{-1}) to salinity dependence for waters from the WTNA. Numbers refer to stations.

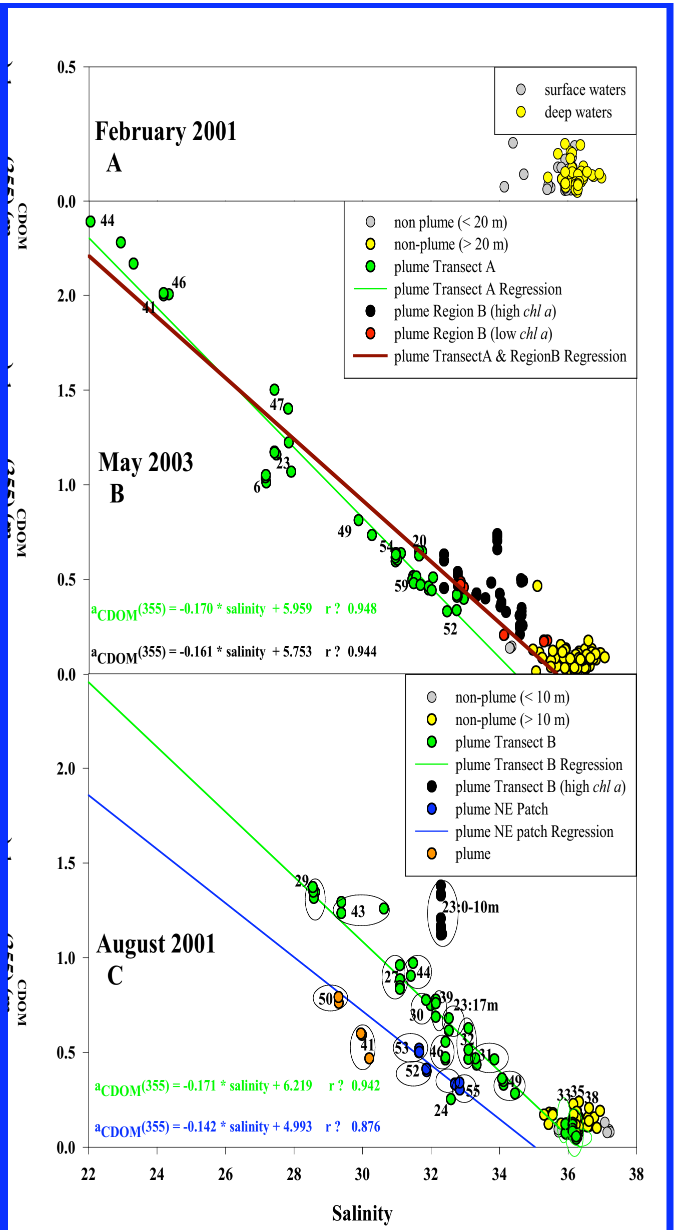

Del Vecchio, R. and A. Subramaniam (2004) Influence of the Amazon River on the surface optical properties of the Western Tropical North Atlantic Ocean. Journal of Geophysical Research. 109, C11001, doi:10.1029/2004JC002503

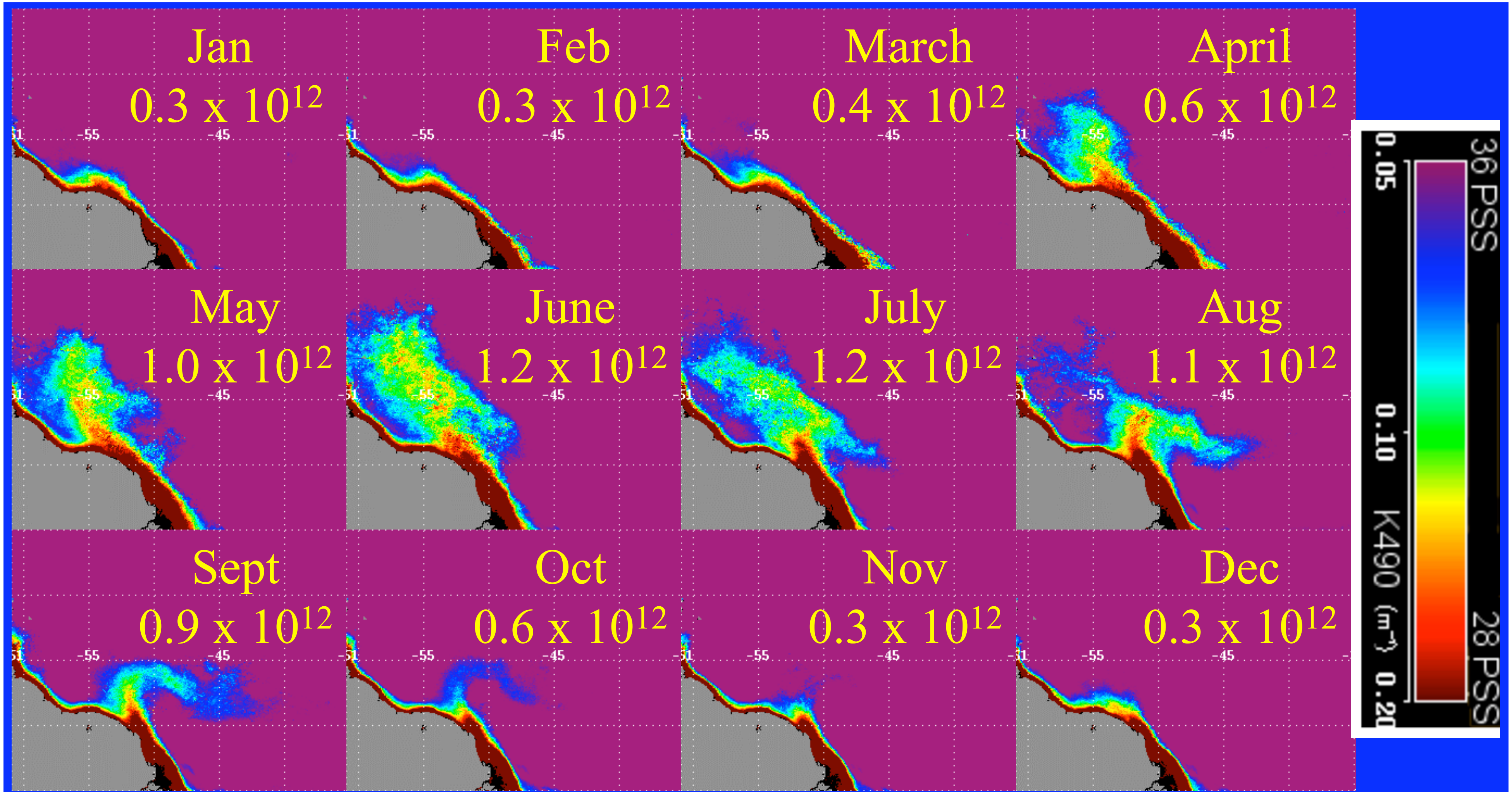

f_{river} for the Amazon calculated using the technique of Muller-Karger et al 1989 was 0.03 for the plume implying that N had to be recycled 39 times to meet the measured primary production demand.

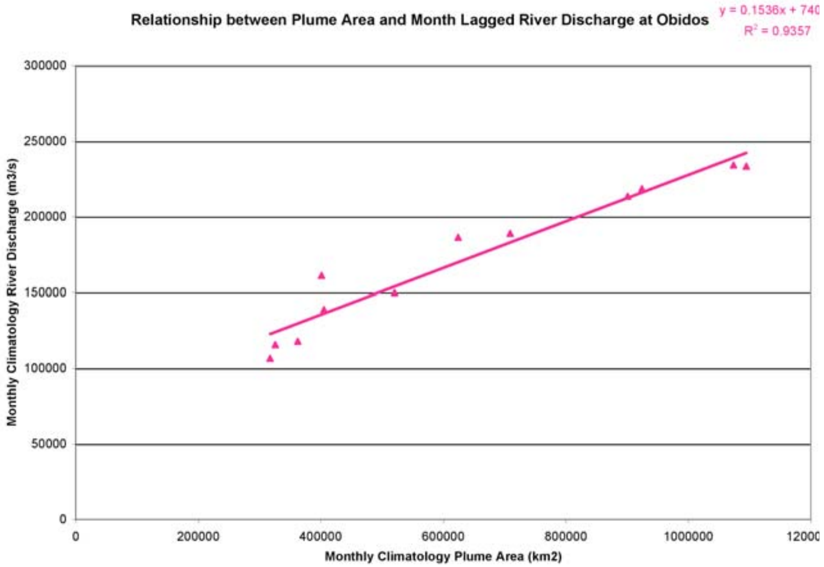

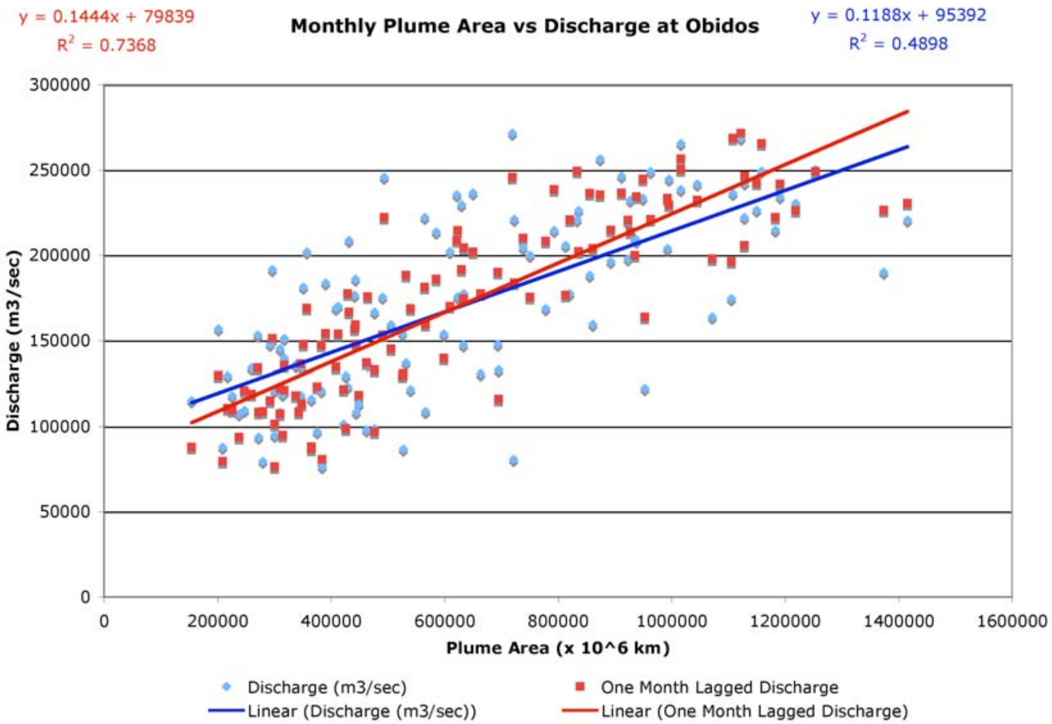

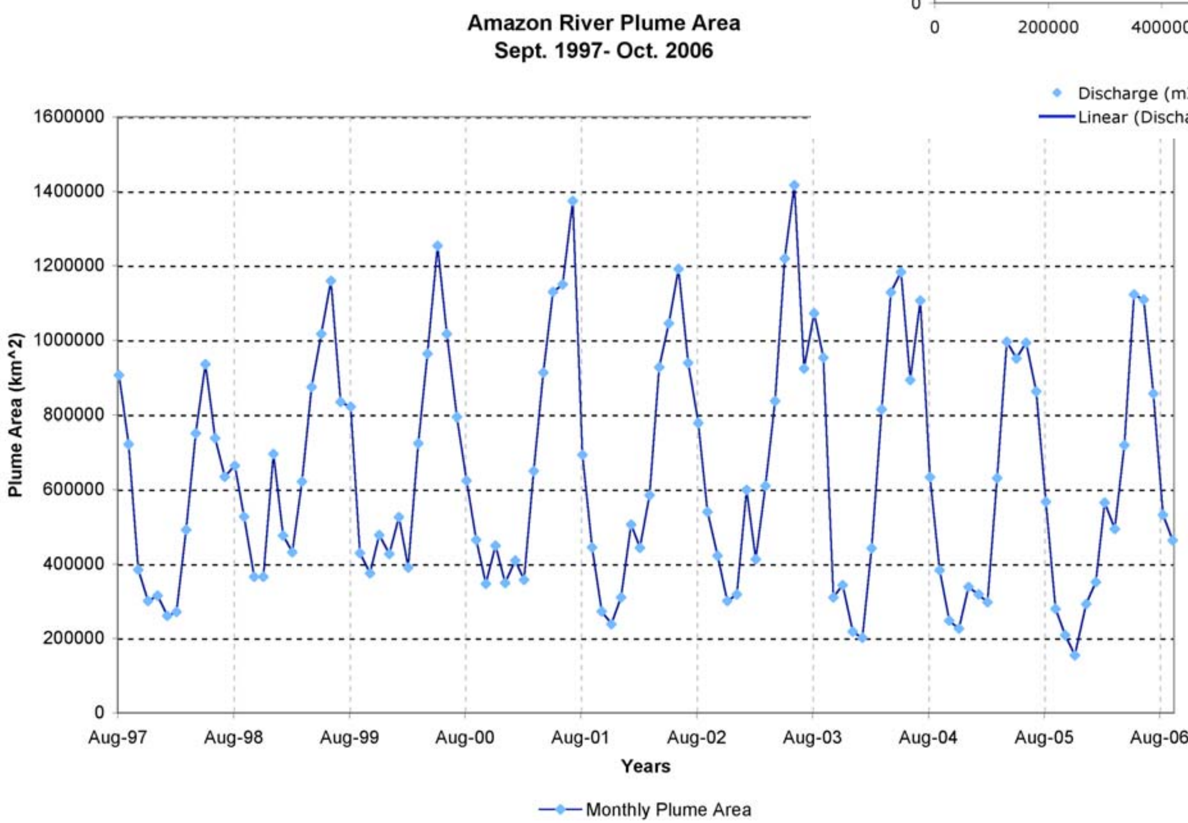

Amazon River Discharge and Climate Variability: 1903 to 1985

JEFFREY E. RICHEY, CARLOS NOBRE, CLARA DESER

Reconstruction of an 83-year record (1903 to 1985) of the discharge of the Amazon River shows that there has been no statistically significant change in discharge over the period of record and that the predominant interannual variability occurs on the 2- to 3-year time scale. Oscillations of river discharge predate significant human influences in the Amazon basin and reflect both extrabasinal and local factors. Cross-spectrum

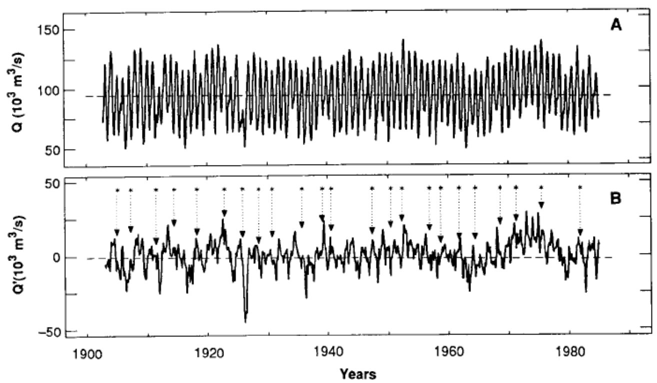

Fig. 2. Discharge of the Amazon River at Manacapurú; (**A**) discharge time series, 1903 to 1985; (**B**) deseasonalized Q′ hydrograph, 1903 to 1985. Arrows indicate occurrence of ENSO events.

Amazon Annual Hydrological Cycle

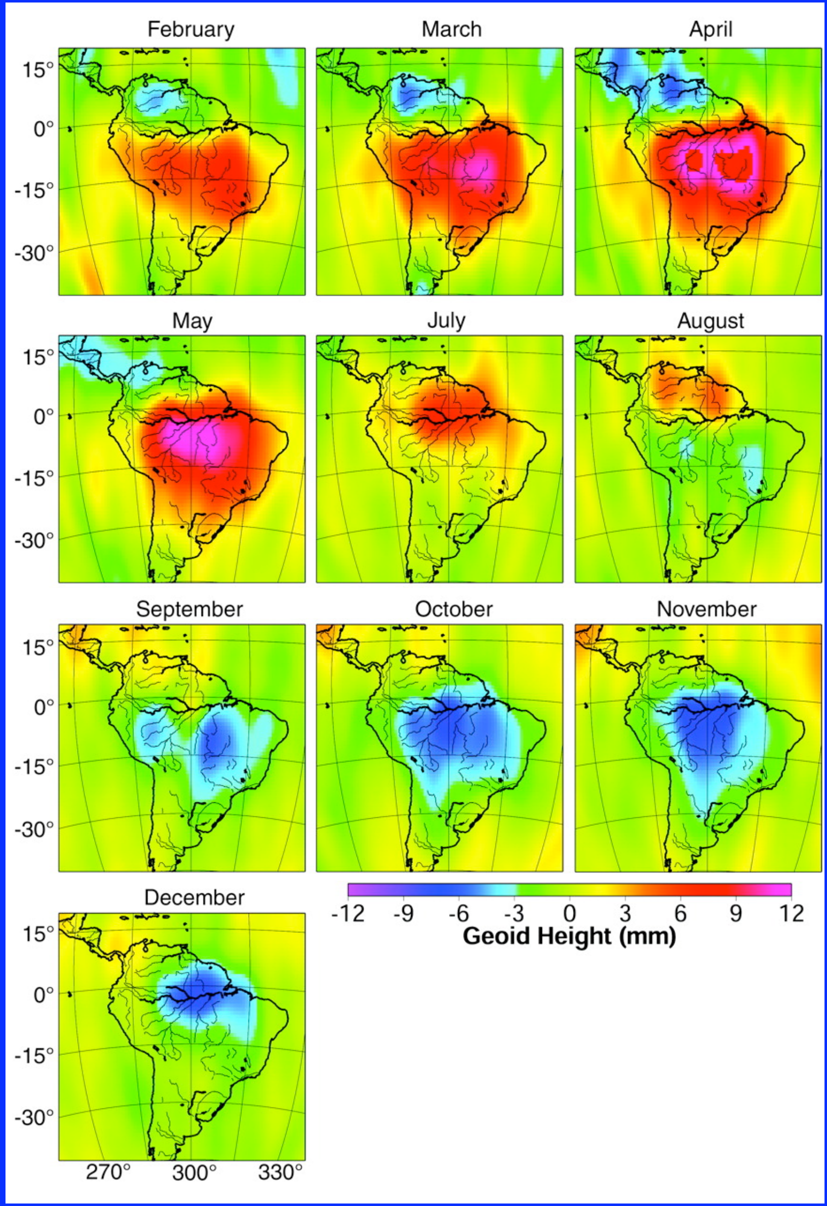

Fig. 2. From Tapley et al 2004 Science

Geoid height differences between each 2003 monthly gravity solution and the 14 month mean for equatorial South America (smoothing radius 400 km; degree-2 coefficients not included). This level of smoothing admits more error from the GRACE estimates, but the large signal in this region allows a higher resolution. Spacecraft events resulted in insufficient ground coverage to resolve the gravity field for the months of January and June.

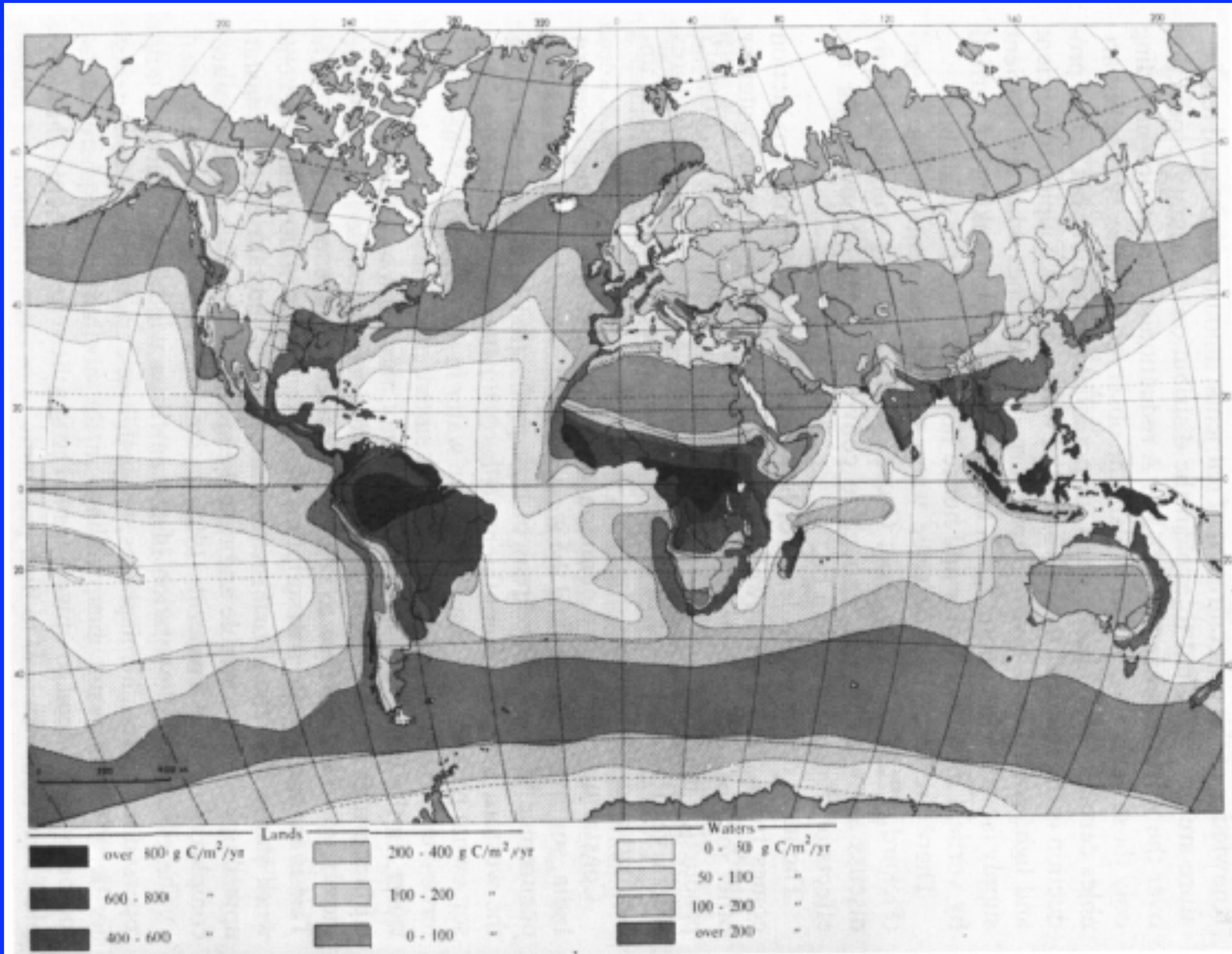

From Lieth (1975)

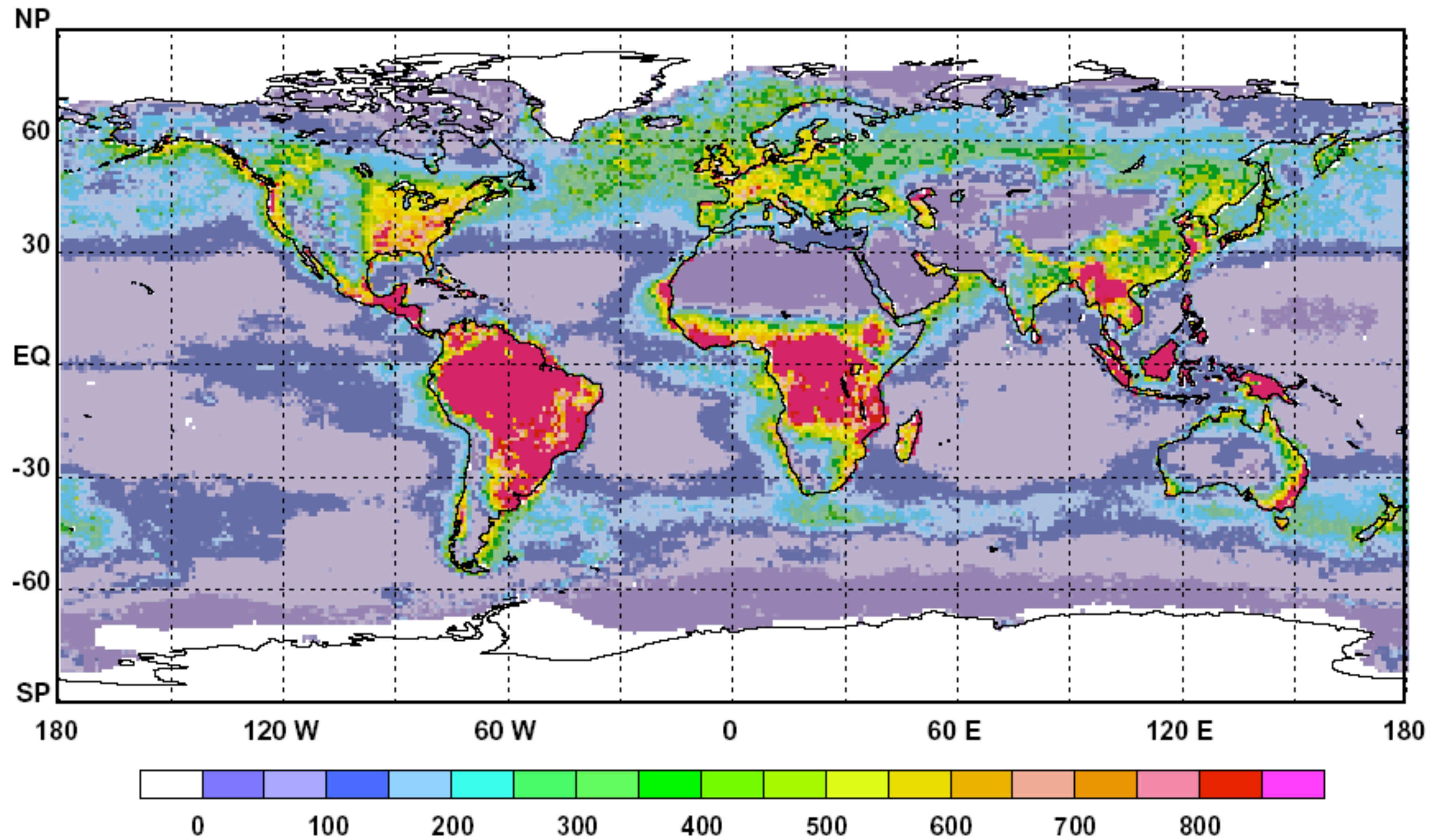

Fig. 1. Global annual NPP (in grams of C per square meter per year) for the biosphere, calculated from the integrated CASA-VGPM model. The spatial resolution of the calculations is 1° 3 1° for land and 1/6° 3 1/6°for the oceans. Input data for ocean color from the CZCS sensor are averages from 1978 to 1983. The land vegetation index from the AVHRR sensors is the average from 1982 to 1990. Global NPP is 104.9 Pg of C year^{-1} (104.9 x 10^{15} g of C year $^{-1}$), with 46.2% contributed by the oceans and 53.8% contributed by the land.

Mar-May

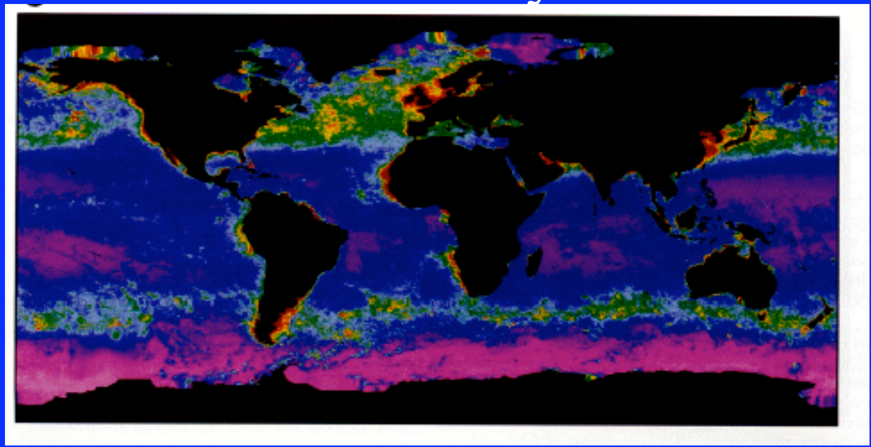

Jun-Aug

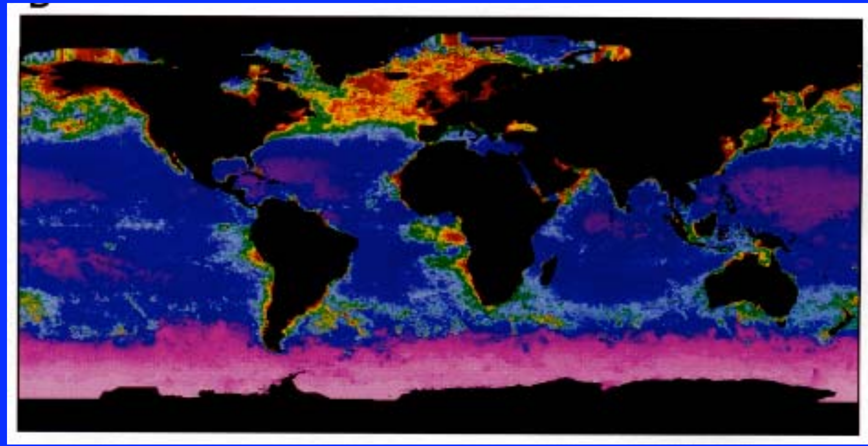

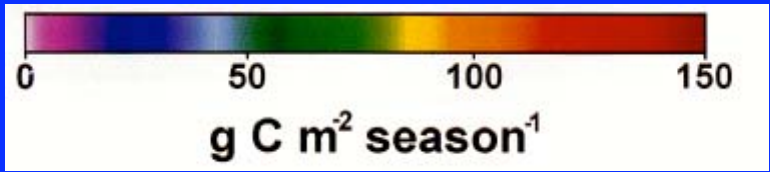

From Behrenfeld and
Falkowski 1997, L&O

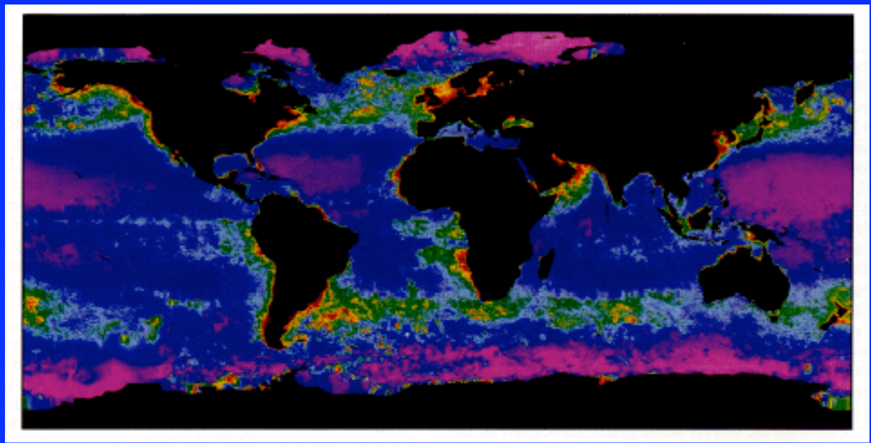

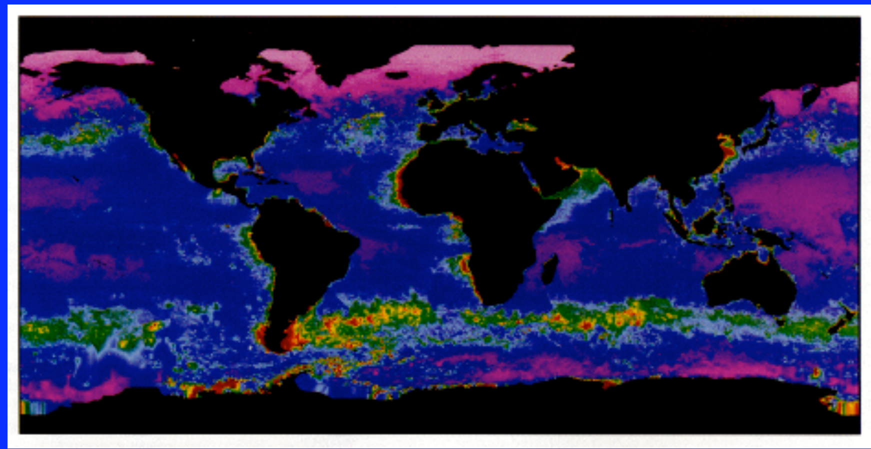

Sep-Nov

Dec-Feb

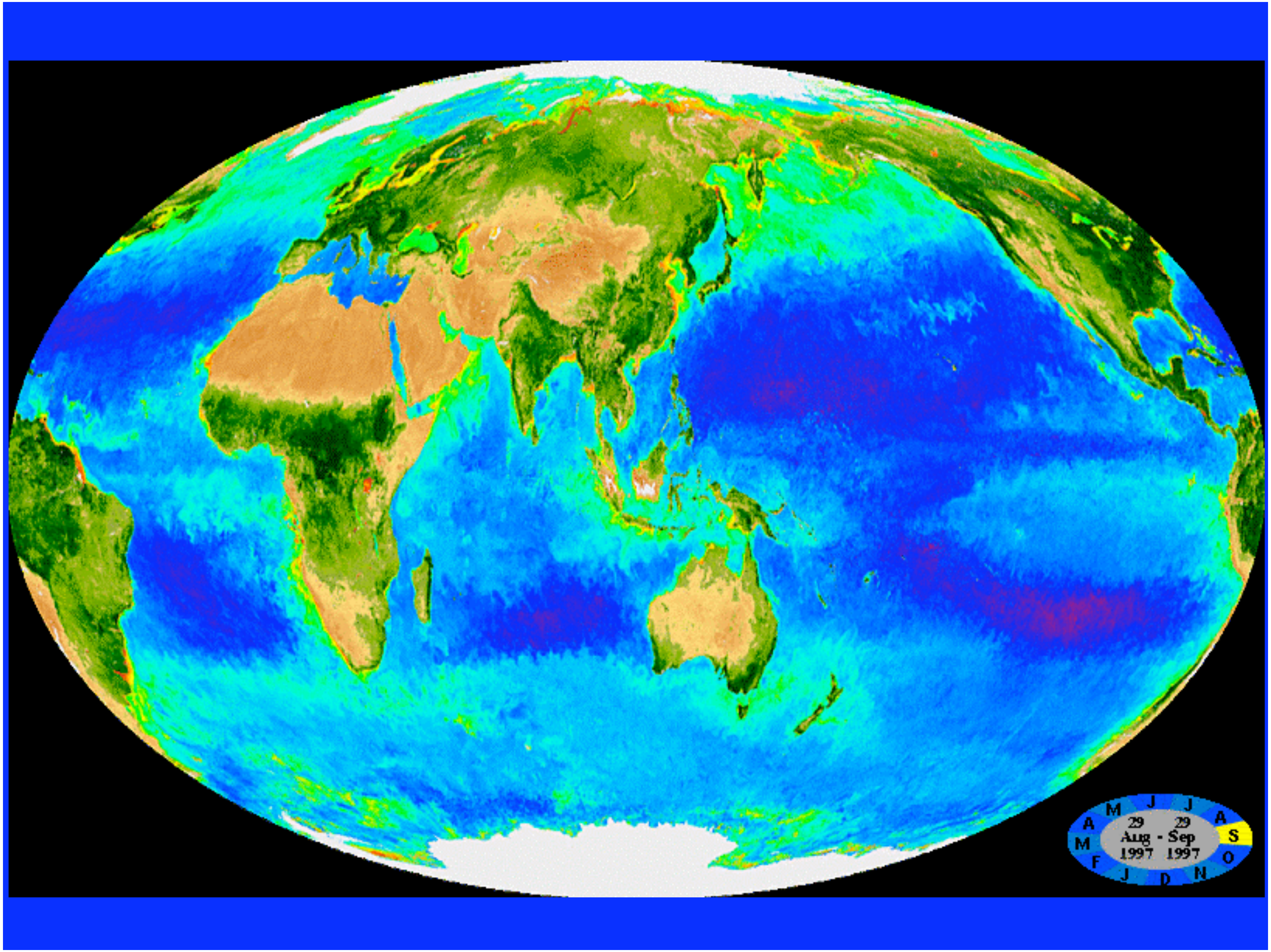

M
J
J
A
A
29
29
Aug - Sep
1997 1997
S
M
F
O
J
D
N

Some useful website sites for more information on ocean color remote sensing:

http://oceancolor.gsfc.nasa.gov/

http://oceancolor.gsfc.nasa.gov/gallery.html

http://visibleearth.nasa.gov/cgi-bin/results?st=1&page=36&th=905&query=seawifs

For the animations go to:

http://www.gsfc.nasa.gov/topstory/20010327colors_of_life.html

http://svs.gsfc.nasa.gov/search/InstrumentsDatasets/SeaStar-SeaWiFS.html